Proteolytic processing of protein tyrosine phosphatase receptor type Z in the CNS

Jeremy Pak Hong Chow

DOCTOR OF

PHILOSOPHY

DEPARTMENT OF BASIC BIOLOGY

SCHOOL OF LIFE SCIENCE

THE GRADUATE UNIVERSITY FOR ADVANCED STUDIES

2008

Table of Contents

Abbreviations……...*i*

Abstract……*ii*

Chapter I Genernal Introduction……...1

I.1 Regulation of protein phosphorylation……2

I.2 Protein tyrosine phosphatase receptor type Z……3

I.3 Ectodamain shedding……9

I.4 Aim of Study……13

Figures……15

Chapter II TACE- And Presenilin/γ-secretase-Mediated Cleavage of Protein Tyrosine Phosphatase Receptor Type Z……..27

II.1 Introduction……28

II.2 Materials and methods……30

II.3 Results……35

II.4 Discussion……43

Figures……47

Chapter III Plasmin-Mediated Processing of Protein Tyrosine Phosphatase Receptor Type Z Is Enhanced after Kainate-Induced Seizures in The Mouse Brain……73

III.1 Introduction……74

III.2 Materials and methods……76

III.3 Results……78

III.4 Discussion……82

Figures……84

Chapter IV Conclusion and Perspectives……94

IV.1 Conclusion and perspectives……95

Figures……97

Acknowledgements……99

References……100

Abbreviations

ADAM	A disintegrin and metalloproteinase
APP	Amyloid precursor protein
Caspr	Contactin associated protein
CNS	Central nervous system
Git1	G protein-coupled receptor kinase interactor 1
GPI	Glycosylphosphatidylinositol
LTP	Long term potentiation
MAGI-1	Membrane-associated guanylate kinase inverted 1
MMP	Matrix metalloproteinase
NMDA	N-methyl-D-aspartic acid
Nr-CAM	Neuronal cell adhesion molecule
PDZ	PSD-95/DLG/ZO-1
PSD95	Postsynaptic density-95
PTK	Protein tyrosine kinase
PTN	Pleiotrophin
PTP	Protein tyrosine phosphatase
Ptprz	Protein tyrosine phosphatase receptor type Z
RhoGAP	Rho-GTPase-activating protein
RIP	Regulated intramembrane proteolysis
TACE	TNF-α converting enzyme
TNF-α	Tumor Necrosis facter-α
tPA	tissue plasminogen activator
X-gal	5-bromo-4-chloro-3-indolyl-beta-D-galactopyranoside

Abstract

Protein tyrosine phosphatase receptor type Z (Ptprz, also known as PTPζ or RPTPβ) is preferentially expressed in the brain as a major chondroitin sulfate proteoglycan. Three splicing variants, two receptor-type isoforms and one secretory isoform, are known. Ptprz interacts with the PSD95 family through its intracellular carboxyl-terminal PDZ-binding motif in the postsynaptic density of the adult brain. *Ptprz*-deficient mice display impairments in spatial and contextual learning. Here, I show that the extracellular region of the receptor isoforms of Ptprz are cleaved by metalloproteinases including ADAM-17 (TACE) and subsequently the membrane-tethered fragment is cleaved by presenilin/γ-secretase, releasing its intracellular region into the cytoplasm: Noteworthily, the intracellular fragment of Ptprz shows nuclear localization. Administration of GM6001, an inhibitor of metalloproteinases, to mice demonstrated the metalloproteinase-mediated cleavage of Ptprz under physiological conditions. Furthermore, I identified the cleavage sites in the extracellular juxtamembrane region of Ptprz by TACE and MMP-9. This is the first evidence of the metalloproteinase-mediated processing of an RPTP in the central nervous system.

I also identified the proteolytic processing of Ptprz by plasmin in the adult mouse brain, which is markedly enhanced after kainate-induced seizures. We estimated the cleavage sites in the extracellular region of Ptprz based on cell-based assays and *in vitro* digestion experiments with recombinant proteins. The findings indicate that Ptprz is a physiological target for activity-dependent proteolytic processing by the tPA/plasmin system, and suggest that the proteolytic fragments are involved in the structural and functional processes of the synapses during learning and memory.

Chapter I

General introduction

I.1 Regulation of protein phosphorylation

Phosphorylation on protein is a fundamental mechanism for cell signaling. By changing the status of phosphorylation on protein, signals are transduced within cells. In particular, phosphorylation on tyrosine is extensively developed in multicellular eukaryotes. It is used to for many cellular events including, cellular mobility, proliferation and differentiation. It also plays role on the coordination of these processes among neighboring cells in embryogenesis, organ development, tissue homeostasis, and the immune system.

Protein tyrosine phosphorylation is controlled by the balance between the activities of protein tyrosine kinases (PTKs) and protein tyrosine phosphatases (PTPs). Proportionally, much more researches have focused on PTKs in the last 20 years. It may be due to the historical reason that the first PTK (Czernilofsky et al., 1980) was cloned 10 years earlier than the first PTP (Guan et al., 1990). There exist 81 active PTPs and 85 active PTKs encoded by human genome (Tonks, 2006). From this similar amount, one can therefore assume that they have comparable significance in cellular signaling. In fact, recent findings have led to the recognition that PTPs play important and active roles in regulating the level of tyrosine phosphorylation.

I.1.1 Receptor-like protein tyrosine phosphatase

Members of PTP super-family are characterized by the presence of a signature motif, H-C-X-X-G-X-X-R (Aloso et al., 2004). Based on the amino acid sequences of their catalytic domain, the PTPs can be divided into two classes: the classical phosphotyrosine (pTyr)-specific phosphatases and the dual specificity phosphatases (for both phosphothreonine and phosphotyrosine). There are 8 subtypes of receptor-like

PTPs (RPTPs) in the class of classical pTyr-specific phosphatase. On the presence of extracellular domains, the RPTPs are presumed to have the potential to regulate cellular activities from external signals. In fact, most of RPTP extracellular domains show features of cell-adhesion molecules, implicating in the processes that involve cell-cell contact. Most of the RPTPs possess two tandem PTP domains in their intracellular regions, the active membrane-proximal PTP domain (named D1) and the inactive membrane-distal PTP domain (named D2) (Tonks, 2006).

I.2 Protein tyrosine phosphatase receptor type Z (Ptprz)

Protein tyrosine phosphatase receptor type Z (Ptprz, also known as PTPζ or RPTPβ) is a RPTP classified in the R5 subfamily, and expressed predominantly in the central nervous system (CNS). Ptprz contains a carbonic anhydrase-like domain, a fibronectin III domain, a serine-glycine rich region, a transmembrane segment and an intracellular region with two tandem PTP domains followed by a PDZ-binding motif in the C-terminus. (Fig. I-2A). In mouse, *Ptprz* gene is located on chromosome 6 and composed of 30 exons. By alternative splicing in the large 12th exon, it is known that three isoforms of Ptprz are generated: the long receptor form Ptprz-A, the short receptor form Ptprz-B with a deletion of 860 amino acid in the serine-glycine rich region, and the secreted form Ptprz-S composed of only the extracellular domain (also known as 6B4 proteoglycan or phosphacan) (Fig. I-2B).

The highly modified extracellular domain with long chains of chondroitin sulfate (CS) and keratin sulfate (KS) is one of the features of Ptprz. It is known that the modification is implicated in protein-protein interaction due to its negative charges. The modifications of Ptprz are developmentally regulated to constitute the sites for the

binding molecules (Nishiwaki, 1998).

I.2.1 Binding molecules to the extracellular region of Ptprz

The complex structural nature of the extracellular domain of Ptprz may repesent a multifunctional protein with various binding molecules. In fact, a list of molecules has been reported to bind to the extracellular domain of Ptprz (Table I-1). Contactin is a GPI-anchored protein expressed exclusively on neuron during development, which is shown to bind to the CAH domain of Ptprz (Peles et al., 1995). The neuronal recognition complex of contactin, Caspr and Nr-CAM (also binds to Ptprz) may induce a signal transduction through the proline-rich region in Caspr to recruit a subset of signaling proteins with SH3 domain and the PDZ-binding motif located at the C-terminus of Nr-CAM.

It has been also shown that Heparin binding growth factors, pleiotrophin (PTN) and midkine, bind to the extracellular region of Ptprz (Maeda et al., 1996, 1999). The high binding affinity of pleiotrophin to Ptprz is abolished by the removal of CS modification. Functionally, immobilized pleiotrophin promotes cell migration, but antibodies against the extracellular region of Ptprz and the removal of the chondroitin sulfate abolish the cell migration-promoting effect. It suggests that pleiotrophin regulates cell migration through Ptprz signaling.

The fact that several molecules have been shown to bind to the extracellular region of Ptprz with different cellular responses make a tempting speculation of ligands –induced regulation of the phosphatase activity in the intracellular region. In the case of receptor-type protein kinases, ligands induced the dimerization of receptor to activate

the kinase activity. However, the regulation mechanism of RPTP is not fully elucidated.

I.2.2 Binding molecules to the intracellular region of Ptprz

The search of binding molecules for Ptprz was first conducted using yeast two-hybrid screening method, in which the whole intracellular region of Ptprz was used as a bait. In the screening, clones encoding PSD95 (post-synaptic density 95) and some other PDZ domain-containing proteins were isolated (Kawachi et al., 1999; Fukada et al., 2005). PSD95 is composed of three PDZ domains, a SH3 domain and a guanylate kinase-like domain. It has diverse synaptic functions, such as interaction with membrane proteins to regulate their synaptic localization. PSD95 seems to stabilize interacting membrane proteins at synapses by suppressing their lateral diffusion or internalization (Bats et al., 2007; Prybylowski et al., 2005; Roche et al., 2001). In addition to its role in protein trafficking, PSD95 regulates the functional properties of interacting membrane proteins, as shown by PSD95-dependent changes in the gating of NMDA receptors (Lin et al., 2006). Interestingly, Ptprz and its subfamily member, Ptprg, are the only two RPTPs containing a PDZ-binding motif in their C-terminal tail. Subcellular fractionation analysis demonstrated that Ptprz is enriched in the PSD fraction (Kawachi et al., 1999). These findings suggest that Ptprz may play role at the synapse.

I.2.3 Substrates for Ptprz

To understand the function of Ptprz, identification of its substrates is essential. However, the traditional yeast two-hybrid screening method has been shown not a good

method for PTP's substrate screening. To this end, some modifications were made. Firstly, a conditional expression of src kinase was introduced to increase the tyrosine phosphorylation level of the substrate molecules. Secondly, a phosphatase activity-impaired mutant (substrate-trapping mutant) was used as a bait to provide a stable association with the substrates. By using the modified yeast two-hybrid system, a list of candidate substrate molecules, including Git1, p190 RhoGAP and MAGI-1, was isolated (Table I-2). Git1 has been found to play role in a wide range of cellular events including vesicular trafficking, cell adhesion and cytoskeleton organization through its ADP-ribosylation factor (ARF)-GTPaes-activating protein (GAP) activity (Kawachi et al., 2001). p190 RhoGAP is a GAP for the Rho family of GTPases and is known to participate in the cytoskeletal organization through the regulation of Rho activity (Chang et al., 1995). Rho family GTPases act as the main regulator of actin cytoskeletal dynamics in a variety of situations including neurite extension, cell migration, cell adhesion, and cell morphological changes (Hall, 1998). MAGI-1 contains a guanylate kinase domain, two WW motifs, and five PDZ domains, and is believed to function as a molecular scaffold in the formation of multiprotein complexes on the cytoplasmic surface of the cell membrane as is PSD-95 (Dobrosotskaya et al., 1997). Interestingly, Ptprz also interacts with the PDZ domain of MAGI-1 through its PDZ-binding motif suggesting that the association with a region other than the PTP domain may mediate its substrate recognition. When cells were stimulated with pleiotrophin, a ligand of Ptprz, the tyrosine phosphorylation level of Git1, p190 RhoGAP and MAGI-1 were increased (Kawachi et al., 2001; Fukada et al., 2006).

I.2.3 Regulation of Ptprz

In a previous study, the crystal structure of the membrane-proximal PTP domain of RPTPα showed that they are organized in a symmetrical dimer, in which an inhibitory wedge motif from one molecule occluded the active site of the other. It has been proposed that the state of dimerization might attenuate the catalytic activity of RPTPs (Bilwes et al., 1996). However, many RPTPs contain two tandem intracellular PTP domains, D1 and D2, instead of one. In two more recent studies on RPTPs, the crystal structures of D1 and D2 domains of CD45 and LAR showed that two domains were tightly packed against each other (Nam et al., 1999). The presence of the D2 might prevent the wedge-mediated dimerization. The PTP domains (D1 and D2) are connected with a transmembrane segment and an extracellular region, which may influence the free orientation of D1 and D2. By using a chimeric mutant comprising the extracellular region of EGF receptor and the intracellular region of CD45, it has been shown that ligand-induced dimerization of this molecule inhibited the function of the RPTP in the regulation of T-cell signaling (Majeti et al., 1998).

In view of the regulation by ligand-induced dimerization, Ptprz is the best characterized example. An acute regulation of Ptprz activity following binding of pleiothrophin has been shown by monitoring the tyrosine phosphorylation level of its substrate molecules. In several separate studies, tyrosine phosphorylation level of substrate molecules, including Git1 and Magi-1, was increased within 30 min after PTN stimulation (Kawachi et al., 2001). PTN was reported to form non-covalent dimer in the presence of heparin or sulfated glycosaminoglycans (Bernard-Pierrot et al., 2005). Therefore, the dimer form of PTN binds to two Ptrpz molecules, and may induce the dimerization of the receptor. In a more recent study, dimerization (or oligomerization)

of Ptprz using an artificial dimerization system leads to the inactivation of the phosphatase. Also, the application of PTN induced the oligomerization of the receptor on the cell surface, and this correlated to the increase tyrosine phosphorylation level of its substrates (Fig. I-4) (Fukada et al., 2006).

I.2.4 Functional role of protein tyrosine phosphatase receptor type Z (Ptprz)

The analyses of the *Ptprz*-deficient mice could provide a clue to understand the physiological function of Ptprz. In 1998, the first line of *Ptprz*-deficient mice was generated. In the knock-out mice, *Ptprz* gene was replaced by LacZ gene (Shitani et al., 1998). Under the control of *Ptprz* gene regulatory unit, LacZ was expressed and visualized by X-gal staining (Fig. I-5). As expected, strong X-gal signal was detected in the CNS. Neurons and astrocytes were found expressing Ptprz. The knockout mice are viable and fertile with no gross anatomical change in the CNS system. The loss of function of Ptprz might be compensated by other RPTPs. An independently generated line of knockout mice also show no obvious abnormality, but a fragility of myelin, in the CNS (Harroch, 2000).

The expression of Ptprz was developmentally regulated (Nishiwaki, 2000). After maturation, high expression level of Ptpz is found in the hippocampus, in which memory is governed (Shitani et al., 1998). The C-terminus of Ptprz binds to PSD95, a well-known scaffold protein in the synapse (Kawachi et al., 1997). In rat brain, they were colocalized in the dendrites of the pyramidal cell in the hippocampus. In the same view, it has been reported that *Ptprz*-deficient mice exhibited impairment of spatial learning in a maturation-manner (Niisato et al., 2005). In the same study, mature Ptprz-deficient mice showed a poor performance in Morris water maze test and

an enhancement of hippocampal long-term potentiation (LTP) (Niisato et al., 2005). In more recent study, *Ptprz*-deficient mice were shown to have impairment in the contextual fear conditioning along with the abnormal tyrosine phosphorylation of its substrate p190 RhoGAP (Tamura et al., 2006).

Apart from the function in the CNS system, Ptprz is also expressed in the stomach. Mice deficient in *Ptprz* is resistant to mucosal damage induced by the vacuolating toxic VacA from *Helicobater pylori* (Fujikawa et al., 2003).

I.3 Protein ectodomain shedding

The release of the extracellular domain through regulated proteolysis is recognized as a general mechanism to control the function of transmembrane proteins (Arribas and Borroto, 2002). This type of proteolysis is known as ectodomain shedding. It affects a large group of type-I transmembrane proteins. Thus, ectodomain shedding might potentially regulate most cellular functions mediated by transmembrane proteins.

Ectodomain shedding occurs near the cell surface. The vast majority of the events are mediated by zinc-dependent metalloproteases. Certain growth factors and cytokines are synthesized as transmembrane forms. Through ectodomain shedding, the receptor-binding domains are released from the cell surface, forming diffusible and functional ligands to their receptors. The most investigated cytokine is Tumor Necrosis facter-α (TNF-α). TNF-α is a type-I transmembrane protein with a short cytoplasmic tail. It primarily involves in systemic inflammation. Ectodomain shedding is required to release the soluble and functional TNF-α from the cell membrane (Wong et al., 1989;Brachmann et al., 1989; Yang et al., 2000).

Besides the transmembrane growth factors, some type-I transmembrane

receptors are also found to be shed. The soluble fragment generated by shedding modulates the function of ligands by preventing the formation of signal complexes. The membrane-tethered fragments left behind are sometimes further cleaved within the transmembrane domain to release the whole intracellular region into the cytosol. This type of proteolytic intramembrane cleavage is known as regulated intramembrane proteolysis (RIP). In some cases, the intracellular fragment translocates to the nucleus, and regulates gene transcription (Arrabis and Borroto, 2002).

Members of the ADAM (a disintegrin and metalloproteinase) family have been identified as proteases that mediate diverse shedding events (Blobel, 2005). The ADAM proteins are type I transmembrance proteins. They possess a propeptide domain, a metalloproteinase domain, a cysteine-rich region, an epidermal growth facter-like sequence, a transmembrane domain, and a cytoplasmic tail. The first member of the ADAM family has been shown to be responsible for a particular shedding event was the TNF-α converting enzyme (TACE, also known as ADAM17), a major sheddase of pro-TNF-α in vivo (Black et al., 1997). To date, TACE has been shown to mediate the shedding of large numbers of molecules. In addition to cytokines and growth factors, TACE also mediates the shedding of membrane receptors. As the most investigated member of the EGFR family, the ligand Neuregulin 1 (NRG1) stimulation of ErbB4 leads to receptor ectodomain shedding by TACE (Rio et al.,, 2000). The membrane-tethered fragment is subsequently cleaved in the transmembrane domain by γ-secretase complexes, releasing its intracellular fragment into the cytosol. The intracellular fragment then translocates into the nucleus (Ni et al., 2001). In a recent study, the intracellular fragment is found to form complex with the signaling protein TAB2 and the corepressor N-CoR in the cytosol, and then translocates

to the nucleus to repress the transcription of glial genes to control the timing of astrogenesis in the developing brain (Fig. I-6) (Sardi et al., 2006)

The matrix metalloproteinases (MMPs) are a large family of zinc-dependent endopeptidases that catalyze the proteolysis of a broad spectrum of extracellular matrix (ECM) and basement membrane protein, including collagens and laminin (Brinckerhoff and Matrisian, 2002; Yong et al., 2001). The MMPs also cleave a range of membrane molecules, including proBDNF and proTNF-α to convert them to their soluble and functional forms (Ethell and Ethell, 2007).

I.3.1 ADAMs and MMPs in the CNS

The studies of ADAMs began in focusing on their role in neurological disorders. Several members of ADAM family serve as α-secretase to increase the level of soluble amyloid precursor protein (APP) and decrease the formation of toxic β-amyloid protein that is involved in Alzheimer's disease (Postina et al., 2004). To get insight into its potential role in neural repair, the importance of ADAMs during development was then intensively studied. The most striking defects are seen in ADAM10-/- mice which die at embryonic day 9.5 with multiple morphological defects in their brains (Hartmann et al., 2002). ADAM10 is the major regulator of proteolytic cleavage of Notch1. Notch activation after the ligand binding requires ectodomain shedding by ADAM10. Subsequently, the cytoplasmic domain is released from the cell membrane for gene regulation, which is needed for cell fate decision of neural progenitor cells (Cornell and Eisen, 2005). The continued expression of ADAMs in the adult CNS suggests that they are also involved in physiological functions (Yang et al., 2006) although little is known about such functions. The role of soluble APP produced by ADAMs in

excitability and synaptic plasticity may provide clues of their functions (Turner et al., 2003). In fact, ADAM10 was detected in the cerebral cortex and hippocampus (Karkkainen et al., 2000), and TACE (ADAM17) was detected in neuron (Skovronsky et al., 2001) and astrocytes (Goddard et al., 2001). Interestingly, TACE was found to bind to SAP97, a scaffold protein in the postsynaptic density (PSD), through the PDZ-binding motif at the C-terminus. However, their roles in synaptic functions are not well elucidated.

Subsets of MMPs are expressed in all cell types of the main nervous like neurons, astrocytes, microglia, oliogodendrocytes, Schwann cells, and neural progenitor cells (Cross and Woodroofe, 1999; Gottschall and Deb, 1996; Ferguson and Muir, 2000; Frolichsthal-Schoeller et al., 1999; Uhm et al., 1998). Some MMPs are secreted into the extracellular space for the structural rearrangement of the ECM. It is now known that the MMPs have roles extending well beyond such physiological and pathological processes. MMP-9, the best characterized MMP, has diverse substrates including matrix and basement membrane molecules such as collagen, in addition to some cytokines and chemokines (Flannery 2006). Formation of new memories requires synaptic reorganization involving extracellular matrix molecules (Dityatev and Schachner, 2003). It has been shown that MMP-9 plays an essential role in learning ability by using the Morris water maze test (Meighan et al., 2006). Also, MMP-9 null mutant mice have defects in hippocampal late-phase long-term LTP (Nagy et al., 2006). However, the detail mechanism of how MMP-9 affects the synaptic plasticity is still not understood.

I.4 Aim of study

Studies on *Ptprz*-deficient mice have shown that Ptprz plays roles in learning and memory formation. *Ptprz*-deficient mice exhibit functional impairments in the hippocampus in a maturation-dependent manner, showing memory deficits in the Morris water maze and enhanced hippocampal LTP in the CA1 region (Niisato et al., 2005). The effect is cancelled out by inhibiting ROCK, a major downstream effector of Rho GTPase (Niisato et al., 2005). In another studies, *Ptprz*-deficient mice show a poor performance in the contextual fear conditioning test together with an abnormal tyrosine phosphorylation level of p190 RhoGAP, a potent inhibitor of Rho GTPase (Settleman, 2003; Tamura et al., 2006). These findings indicate the involvement of Ptprz in p190 RhoGAP-Rho-ROCK pathway in memory formation. However, the direct role of Ptprz in the pathway is not fully elucidated. Ptprz is concentrated in the PSD fractionation through its PDZ-binding motif in the C-terminal tail. The localization of Ptprz suggests its direct role in the central synapse.

There exists three different alternative spicing isoforms of Ptprz in the brain. However, several unidentified low molecular weight species have been detected in western blotting with specific antibodies against the extracellular region of Ptprz (Shitani et al., 1998). Proteolytic processing plays an important role in synaptic plasticity. It has been shown that enzymes involved in proteolysis are essential in memory formation. Taken together, these findings provide clues whether Ptprz is regulated by proteolytic processing including ectodomain shedding in synaptic plasticity and memory formation. In this project, I aim to:

1. characterize the fragments of Ptprz by proteolytic processing.
2. identify proteases that involved in the processing and its molecular mechanism.

Working out the proteolytic processing of Ptprz would be the first step to understand its function in memory formation.

Fig. I-1. Receptor-like protein tyrosine phosphatase. Receptor-like PTPs (RPTP) contains two intracellular PTP domains, in which the membrane-proximal D1 domain is catalytically active. In receptor subtype R4, PTPα is unique among the RPTPs in that the membrane-distal D2 domain also displays a low residual activity. For the remaining RPTPs, the D2 domain maintains a PTP fold but lacks activity and can be classified as a pseudophosphatase domain. In each case, the PTPs have been designated by a name that is commonly used in the literature. Where this differs from the gene symbol, the latter is included in parentheses for clarification. In each case, the various subdivisions are based upon sequence similarity.

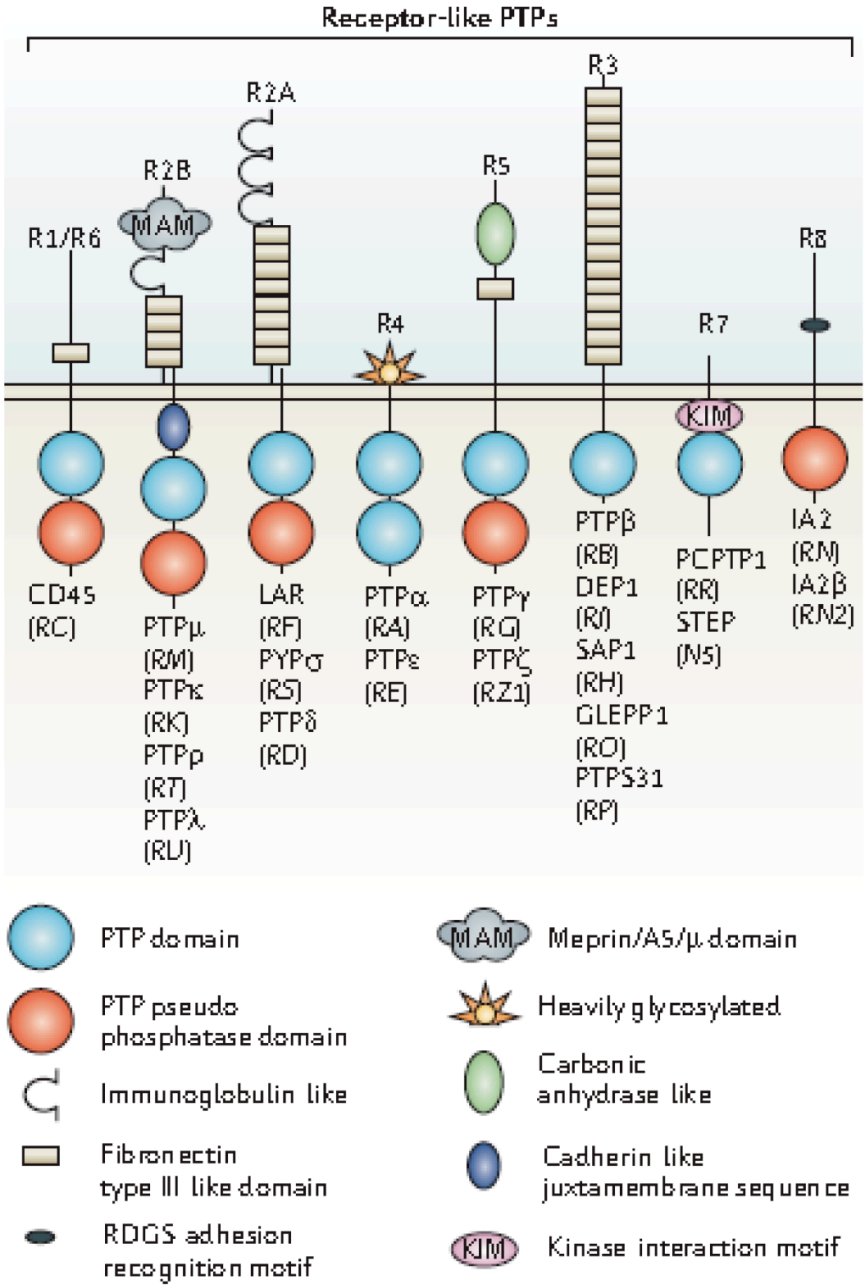

Adapted from Tonks, Nat Rev Mol Cell Biol,7:833-846, 2006 with modification

Fig.I-2. Schematic representation of Ptprz isoforms. A, Schematic representation of Ptprz isoforms with their apparent molecular sizes. Molecular sizes of the chondroitin sulfate (CS) proteoglycan forms (CS-PG) and their core proteins after treatments with chondroitinase ABC (chABC) are shown (Nishiwaki et al., 1998). Regions corresponding to the epitopes of antibodies used in this study are indicated by vertical bars. B, Schematic drawings of the structure of mouse *Ptprz* gene and exon usage in their transcripts. Mouse genome DNA is represented with a horizontal bar, and the exons are depicted as squares with the exon number (upper). *Ptprz* transcripts are shown (lower) with domain structures colored as in A. Domains are highlighted in different colors: CAH, carbonic anhydrase-like domain; FNIII, fibronectin type III domain; PTP-D1 and PTP-D2, tyrosine phosphatase domains.

A

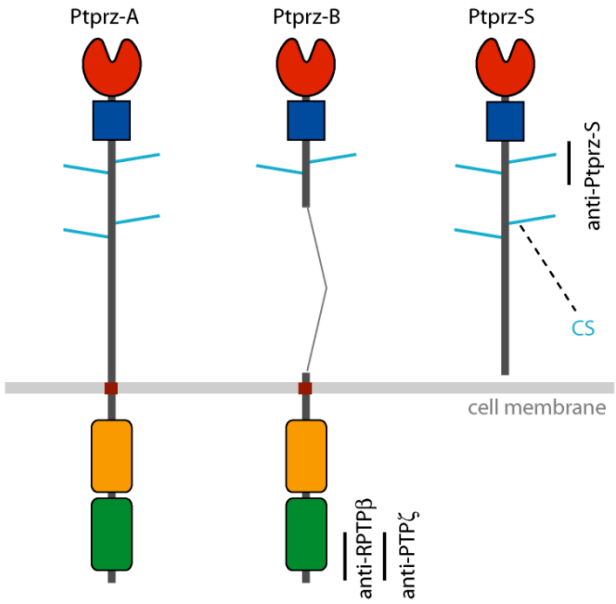

core proteins, kDa	400	250	300
CS-PG forms, kDa	600 -1000	400	600 -1000

B

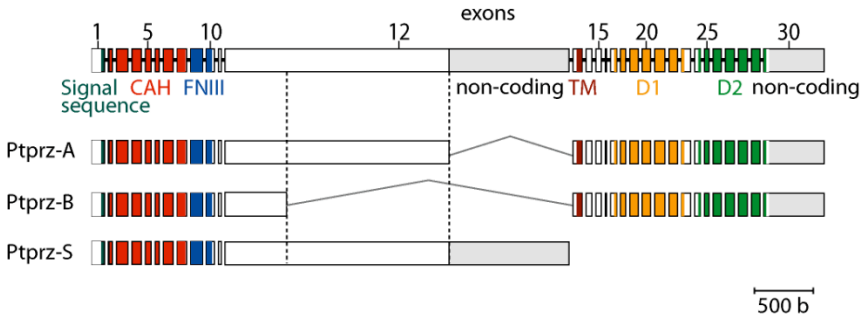

Table I-1. List of molecules reported to bind to the excellular domain of Ptprz

Name	Synonyms	Full-length name
Heparin-binding growth factor		
PTN	NEGF1,HBNF,HB-GAM, HBBN, HBGF-8, HARP, Osf-1, Osf1	pleiotrophin (heparin binding growth factor 8, neurite growth-promoting factor 1)
MDK	NEGF2,Mek, MK	midkine (neurite growth-promoting factor 2)
FGF2	FGFB,bFGF, Fgf-2, Fgfb	fibroblast growth factor 2 (basic)
Extracellular matrix protein		
TNC	Hxb, Ten, TN, TN-C	tenascin C (hexabrachion)
TNR	janusin, restrictin, TN-R	tenascin R (restrictin, janusin)
glycosylphosphatidyl inositol (GPI)-anchored molecule		
CNTN1	F3,CNTN, F3cam	contactin 1
CNTN2	TAG-1, TAX1, AXT,axonin,Tax	contactin 2 (axonal)
Cell adhesion molecules		
NCAM1	NCAM, CD56,E-NCAM, NCAM-1, NCAM-120, NCAM-140, NCAM-180	neural cell adhesion molecule 1
NRCAM	Bravo	neuronal cell adhesion molecule
L1CAM	HSAS1, SPG1, HSAS, MASA, MIC5, S10, CD171,L1	L1 cell adhesion molecule
Other (exogenous)		
VacA*	-	vacuolating cytotoxin

*VacA is a cytotoxin, which is produced by Helicobacter pylori

Table I-2. List of Substrates and interacting molecules of intrcellular domain of Ptprz

Name	Synonyms	Full-length name	Category	Interaction
Substrate (candidate)				
GIT1	Cat-1, p95Cat	G protein-coupled receptor kinase interactor 1	ArfGAP	pTyr
GRLF1	P190 RhoGAP	glucocorticoid receptor DNA binding factor 1	RhoGAP	pTyr
GOPC	PIST, FIG, GOPC1, CAL	golgi associated PDZ and coiled-coil motif containing	PDZ protein	pTyr
MAGI1	BAP1, MAGI-1, TNRC19, AIP3, WWP3,Baiap1, Gukmi1	membrane associated guanylate kinase, WW and PDZ domain containing 1	PDZ protein	pTyr & PDZ
CTNNB1	CTNNB,beta-catenin	catenin (cadherin-associated protein), beta 1, 88kDa	Catenin	N.D
SCN1A		sodium channel, voltage-gated, type I, alpha	Channel	N.D
Intracellular binding molecules (PDZ proteins)				
DLG4	PSD-95, SAP90	discs, large homolog 4 (Drosophila)		PDZ
MAGI3	MAGI-3	membrane associated guanylate kinase, WW and PDZ domain containing 3		PDZ
LIN7C	MALS-3, Lin7c, LIN-7C, VELI3,MALS-3,	lin-7 homolog C (C. elegans)		PDZ
SYNJ2BP	Arip2,ARIP2, OMP25	synaptojanin 2 binding protein		PDZ
SNTA1	SNT1	syntrophin, alpha 1 (dystrophin-associated protein A1, 59kDa, acidic component)		PDZ
SNTB1	59-DAP, A1B, BSYN2, TIP-43, SNT2	syntrophin, beta 1 (dystrophin-associated protein A1, 59kDa, basic component 1)		PDZ
MPDZ	MUPP1	multiple PDZ domain protein		PDZ
Intracellular binding molecules (non-PDZ proteins)				
TNNT2	cardiac TnT	troponin T2, cardiac	Troponin	N.D.
CENTG1	Centg1,Pike, KIAA0167	centaurin, gamma 1	GTPase	N.D.
ABCA12	DKFZP434G232	ATP-binding cassette, sub-family A (ABC1), member 12	ABC transporter	N.D.
SPOP	TEF2,Pcif1	speckle-type POZ protein	E3 ubiquitin ligase	N.D.
SCN1B		sodium channel, voltage-gated, type I, beta	Channel	N.D

Fig. I-4. PTN inactivates Ptprz and induces clustering of Ptprz. A,PTN treatment (100 ng/ml, 1 h) increased the tyrosine phosphorylation of Git1 in cells expressing the wild-type Ptprz-B (WT), but not in mock-transfected (Mock) or PTP-inactive DA mutant of Ptprz-B (DA)-transfected cells (upper). Signal intensities were quantified and expressed below as the percentage compared with the vehicle-treated control of mock-transfected cells (control cells, lane 1). Data are presented as the means ± S.E. (n = 3). **P < 0.01, as compared with control cells. ##P < 0.01, as compared between vehicle and PTN treatments. Ptprz-B expression was confirmed equal using cell lysates without chondroitinase ABC treatment by Western blotting with anti-Ptprz-S antibody (lower). B, Localization of Ptprz-B after treatment with PTN. A patchy distribution of Ptprz-B on the surface was found in PTN-treated (100 ng/ml, 1 h) cells (right; arrowheads), whereas a diffuse distribution was observed in control cells (left). Top, fluorescent images (inverted grayscale); middle, enlargements of the area enclosed by a square in the top panels; bottom, differential interference contrast (DIC) images. Scale bars, 20 μm.

A

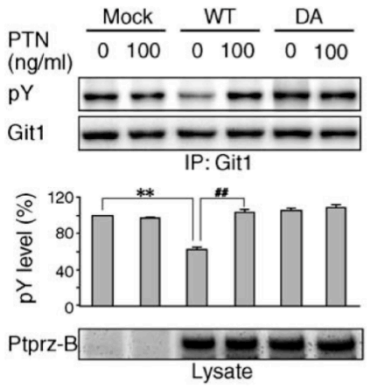

B

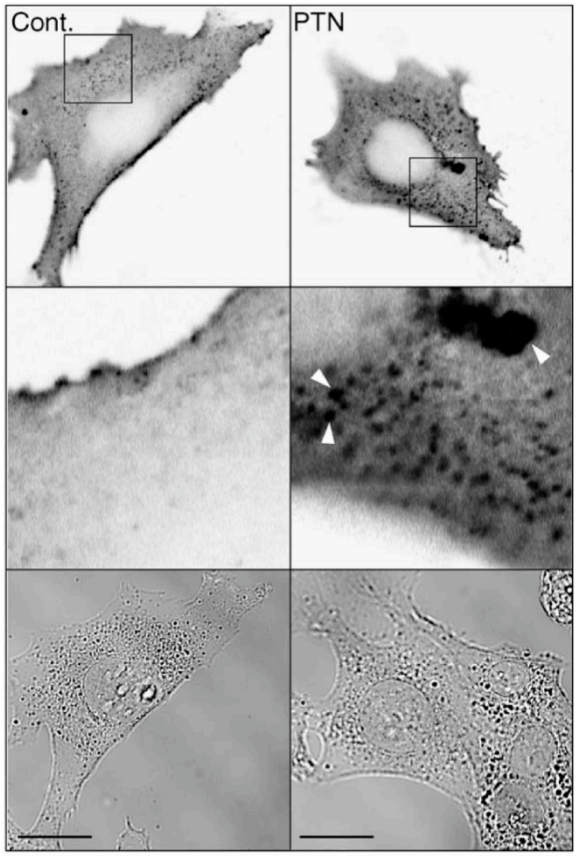

Adapted from Fukada et al, FEBS lett 580:4051–4056, 2006

Fig. I-5. *Ptprz* gene targeting. A, Schematic representation of the structures of the endogenous allele (genomic), the targeting vector (vector) andtargeted allele (targeted). B, BamHI; E, EcoRI; P, PstI. The coding region of *Ptprz* is indicated by the hatched box. For construction of the targeting vector, a 0.6-kb PstI fragment covering the 3' end of exon 1 and the 5' end of intron 1 was replaced with the LacZ-Neo cassette to disrupt the *Ptprz* gene, and the DT-A cassette was placed at the 3' terminal of homologous region for negative selection. The region used as a probe for Southern blotting is indicated by a bar. B, Southern blotting analysis of BamHI-digested genomic DNA from wild-type (lane 1), $Ptprz^{+/-}$(lane 2) and $Ptprz^{-/-}$ (lane 3) mice. Sizes of the wild-type (18 kb) and targeted (8 kb) alleles are indicated on the left. C, Western blotting analysis of the brain membrane fractions from adult wild-type (lane 1) and $Ptprz^{-/-}$ mice (lane 2) using anti-6B4 proteoglycan polyclonal antibody which recognized the extracellular domain of Ptprz. Before electrophoresis, samples were treated with chondroitinase ABC to remove chondroitin sulfate chains. The positions of Ptprz isoforms are shown on the right. Ptprz -A was not detected because it is a minor component in the adult brain. The 120-kDa band was non-specific because it appeared only with the second antibody. Molecular mass markers are indicated in kD on the left. D, X-gal staining of whole-mount E8.5 $Ptprz^{+/-}$ embryo preparations. F and N indicate the forebrain and neural fold, respectively. Scale bar, 400 mm. E, X-gal staining of whole-mount E12.5 $Ptprz^{+/-}$ embryo preparations. Scale bar, 1 mm. F, Identification of LacZ-expressing cells in brain sections from $Ptprz^{+/-}$ mice. p and g indicate the pyramidal cell layer and granule cell layer, respectively. Scale Bar, 200 μm.

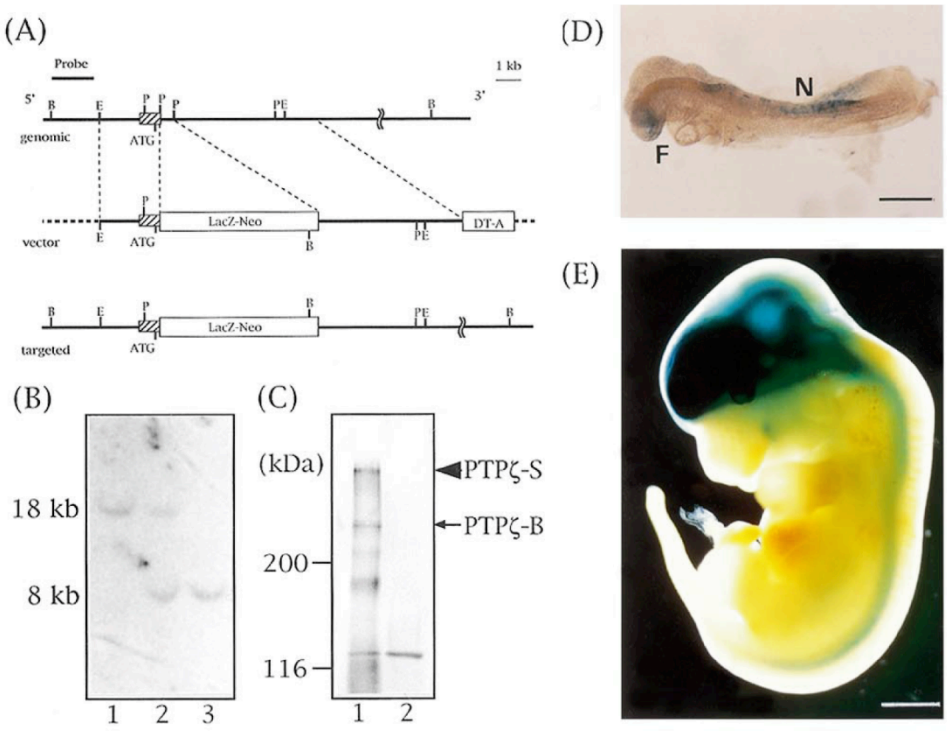

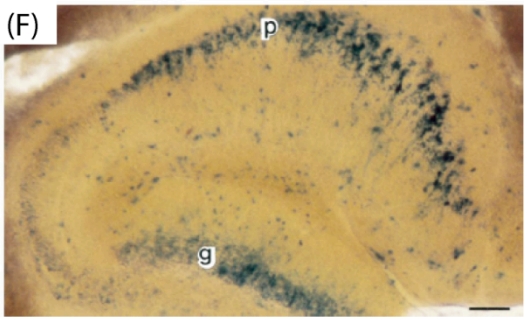

adapted from Shintani et al,Neuro Lett 247:135-138, 2000

Fig. I-6. Ectodomain shedding of cytokines and receptors. (1) The activation of cytokines (TNF-α is used for an example) requires the release of the receptor-binding domain (TNF-α). TACE (ADAM17) mediates the cleavage of proTNF-α within its membrane-proximal (juxtamembrane) region to release the soluble receptor-binding domain from the cell membrane. TNF-α is then able to bind to its receptor, TNFR, located on the same cell or cells at a distance. (2) TACE also mediates the ectodomain shedding of some receptor proteins (ErbB4 is used as an example) to release their extracellular regions. Subsequently, the membrane-tethered counterpart is cleaved by γ-secretase to produce ErbB4-intracellular domain (E4ICD). This type of proteolytic intramembranous cleavage is known as regulated intramembrane proteolysis (RIP). E4ICD can then form a ternary complex and translocate to the nucleus to repress gene transcription that are required for astrogenesis.

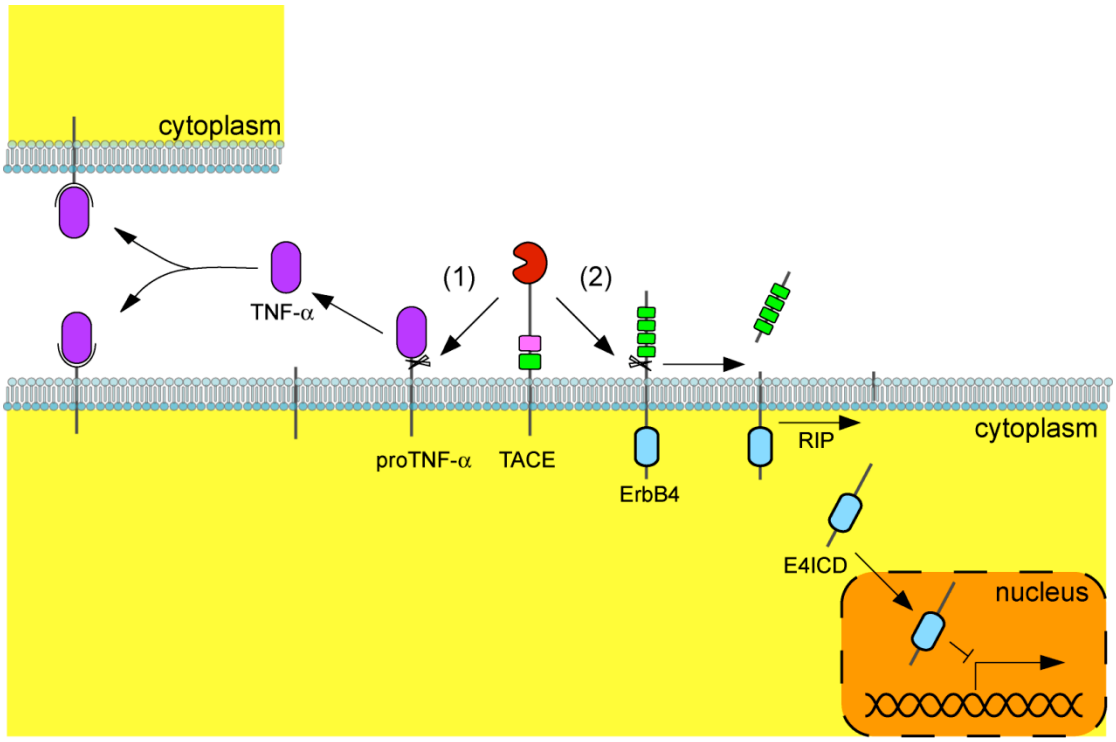
cytoplasm
TNF-α
(1)
(2)
proTNF-α
TACE
ErbB4
RIP
cytoplasm
E4ICD
nucleus

Chapter II

TACE- and Presenilin/γ-secretase-mediated cleavage of protein tyrosine phosphatase receptor type Z

II.1 Introduction

Receptor-type protein tyrosine phosphatases (RPTPs) are a structurally and functionally diverse family of enzymes comprised of eight subfamilies (Tonk, 2006). Protein tyrosine phosphatase receptor type Z (Ptprz, also called PTPζ or RPTPβ) is a RPTP classified in the R5 subfamily, and expressed predominantly in the central nervous system (CNS) (Levy et al., 1993; Nishiwaki et al., 1998). The physiological importance of this protein has been demonstrated through studies of *Ptprz*-deficient mice (Shitani et al., 1998; Fujikawa et al., 2003), which display impairments in hippocampal function in a maturation-dependent manner (Niisato et al., 2005; Tamura et al., 2006). An independently generated knockout-mouse line suggests a fragility of myelin in the CNS (Harroch et al., 2000).

It is known that three isoforms of Ptprz are generated by alternative splicing from a single *Ptprz* gene (on mouse chromosome 6; human chromosome 7): The two transmembrane isoforms, Ptprz-A and Ptprz-B, and the secretory isoform, Ptprz-S (also known as 6B4 proteoglycan or phosphacan) (Levy et al., 1993;Krueger et al., 1992;Maeda et al., 1994; Maurel et al., 1994; Sakurai et al., 1996), all of which are expressed as chondroitin sulfate proteoglycans in the brain (Nishiwaki et al., 1998). However, some inexplicable issues about the molecular profiles of Ptprz have remained in previous studies. For instance, although there exists substantial expression of the respective transcripts for all isoforms (Maurel et al., 1994, Canoll et al., 1996), full-length Ptprz-A has been scarcely observed at the protein level in the adult brain (Nishiwaki et al., 1998). In addition, several lower molecular species have been detected with specific antibodies against Ptprz in wild-type mice (Shitani et al., 1998). The technical difficulty in removal of the chondroitin sulfate chains to separate their

core proteins by SDS-PAGE may induce variability in the signal patterns of this molecule in Western blotting among researchers.

In this study, I examined the molecular profile of Ptprz in the adult CNS tissues at both protein and mRNA levels in detail, and revealed that the proteolytic fragments are abundantly accumulated in the adult mouse brain. The two receptor isoforms were found to undergo ectodomain cleavage by metalloproteinases, releasing their extracellular fragments. The membrane-tethered fragment of Ptprz was further cleaved by presenilin/γ-secretase to release the intracellular fragment, which was consequently detected in the cytoplasm and nucleus. These findings suggest a novel signaling mechanism of Ptprz by the regulated proteolytic processing in the brain.

II.2 Materials and methods

Pharmacological reagents

Phorbol 12-myristate 13-acetate (PMA) was purchased from Sigma. GM6001, compound E, lactacystin, and recombinant TACE were from Calbiochem.

Animal experiments

Adult wild-type and *Ptprz*-deficient mice (Shitani et al., 1998) backcrossed with the inbred C57BL/6 strain for more than ten generations were used. Mice were administered GM6001 suspended in saline containing 1.5% carboxy methyl cellulose (CMC) intraperitoneally (100 mg per kg body weight) as described (Wang et al., 2005). Tissues were isolated at indicated time points after the administration. All animal experiments were performed according to the guidelines of Animal Care with approval by the Committee for Animal Research, National Institutes of Natural Sciences.

Intraventricular infusion of GM6001

Anaesthetized wild-type mice were placed in a stereotzxic apparatus, and brain infusion cannulae (Brain infusion kit 3, Alza Corp.) were inserted in the cerebral ventricle. The cannulae was secured to the skull with an anchoring screw and dental cement. The stereotaxic coordinates were 0.5 mm anterior and 1,0 mm lateral to the bregma, and 2,4 mm below the skull surface. Osmotic mini-pump (Model 1007D, flow rate =0.5 μl per hr, alza Corp,) filled with 2,5 mM GM6001 in 50% DMSO (or the vehicle) was implanted between the scapulae, and connected to the infusion cannulae. After 4 days, the brain were separayed as decribed (Glowinski and Inverson, 1966).

Expression constructs for Ptprz isoforms

Full-length rat Ptprz-A and Ptprz-S (Maeda et al., 1994) were subcloned into the expression vector pZeoSV2 (Invitrogen), to yield pZeo-PTPζ-A and pZeo-PTPζ-S, respectively. The expression plasmid for rat Ptprz-B (pZeo-PTPζ) was described previously (Kawachi et al., 2001). This construct was used as a template to generate pZeo-PTPζ-G1631I (a mutant in which glycine at 1631 is substituted with isoleucine) by using a QuickChange Multi Site-Directed Mutagenesis Kit (Stratagene). The expression plasmid (pZeoSV-PtprzICR) for the entire intracellular region of rat Ptprz-A/B (amino acid residues 1665-2316; GenBank accession number U09357) was prepared by PCR from pZeo-PTPζ using an initiative methionine encoding primer and cloning the fragment into the *Not*I site of pZeoSV2.

Cell Culture and DNA Transfection

HEK293T cells (human embryonic kidney epithelial cells) were grown and maintained on dishes coated with rat tail collagen in Dulbecco's modified Eagle's medium (DMEM) supplemented with 10% fetal bovine serum (FCS) in a humidified incubator at 37˚C with 5% CO_2. HEK293 cell lines stably expressing either human wild-type presenilin 1 (PS1 WT) or a dominant-negative PS1 variant (substitution of Asp at 385 for Ala, PS1 D385A) (Kasuga et al., 2007) were kindly provided by Takeshi Ikeuchi (Niigata University, Niigata, Japan). These cells were transfected with Ptprz expression plasmids by calcium-phosphate precipitation as described (Fujikawa et al., 2007).

CHO-M2, CHO-(M2+TACE) (CHO-M2 cells rescued by expression of TACE), and parental CHO-WT cells (Borroto et al., 2003) were kindly provided by Joaquín

Arribas (University Hospital Vall d'Hebron, Barcelona, Spain). CHO-M2 and CHO-WT cells were maintained in DMEM supplemented with 10% FCS and 500 μg/ml of G418. CHO-(M2+TACE) cells were maintained with G418 and Hygromicin (500 μg/ml of each). These CHO cells were transfected by using Lipofectamine Plus reagent (Invitrogen; 1 μg of plasmid per 3.5-cm dish). Transfected cells were replated once on 3.5-cm dishes, cultured for 24 hr, and then used for the experiments.

Protein extraction and chABC treatment

Mouse tissues quickly separated on ice were homogenized with more than 10 volumes of a lysis buffer: 20 mM Tris-HCl, pH 8.0, 1% NP-40, 137 mM NaCl, 10 mM NaF, 1 mM sodium orthovanadate, and a EDTA-free protease inhibitor cocktail (complete EDTA-free, Roche). Supernatants were then collected by centrifugation at 15,000 *g* for 15 min. Cultured cells were extracted with the same lysis buffer (300 μl per 3.5 cm dish) as above. The samples were stored at -85°C prior to use.

For chondroitinase ABC (chABC) digestion, the protein concentration of each sample was adjusted with the lysis buffer (<4 mg/ml). Aliquots (10 μl) were then incubated with an equal volume of 0.2 M Tris-HCl, 4 mM sodium-acetate, pH 7.5 with or without chABC (Seikagaku Co., Tokyo, Japan, the enzyme was added at 60 μU per μg protein) for 1 hr at 37°C. Protein concentrations were determined with a Micro BCA Protein Assay kit (Pierce).

Western blot analysis

Samples were mixed with an equal volume of 2x SDS-PAGE sample buffer (containing 4% mercaptoethanol), boiled for 5 min, and then separated on a 5-20% gradient

polyacrylamide gel (E-R520L, Atto Corporation, Tokyo, Japan). Proteins were transferred to a polyvinylidene difluoride (PVDF) membrane (Millipore) for 1 hr using a conventional semi-dry electrotransfer (1.3 mA per cm^2). The membrane was incubated for 1 hr in a blocking solution (4 % non-fat dry milk and 0.1 % Triton X-100 in 10 mM Tris-HCl, pH 7.4, 150 mM NaCl), and incubated overnight with anti-Ptprz-S rabbit serum (1:10,000) (Nishiwaki et al., 1998) in the blocking solution supplemented with 0.04% SDS to prevent nonspecific binding. Mouse monoclonal anti-RPTPβ (epitope region is amino acid residues 2098-2307 of human Ptprz-A, 250 ng/ml, BD Biosciences) was incubated with the blots in the blocking solution. The binding of these antibodies was detected with an ECL Western blotting system (GE Healthcare).

Northern blot analysis

Total RNA was isolated from mouse tissues using TRIzol (Invitrogen) and then poly(A)$^+$ RNA was purified using the Dynabeads mRNA purification kit (Dynal) according to the manufacturer's instructions. Northern blotting was performed as described (Suzuki et al., 2000) with slight modifications in the electrophoresis. The poly(A)$^+$ RNA was denatured in 1x MOPS buffer (20 mM MOPS, 2 mM sodium acetate, and 1 mM EDTA, pH 7.0) containing 6.8% formaldehyde, 50% formamide, and 50 μg/ml of ethidium bromide at 67°C for 10 min, chilled on ice for 5 min, and then added with 2.5 μl of a loading buffer (50% glycerol, 0.25% bromophenol blue, and 0.25% xylene cyanol). Electrophoresis was performed on a formaldehyde-denatured agarose gel (6.8% formaldehyde and 1% agarose in 1x MOPS buffer) at 5 V/cm for 4 hr with the circulation of an electrophoresis buffer (6.8% formaldehyde in 1x MOPS buffer).

Templates of complementary DNA probes were as follows: CAH-FNIII probe (nucleotide residues 93-1215 for rat Ptprz-A; GenBank accession number U09357), PTP-D1 probe (nucleotide residues 5047-6081 for rat Ptprz-A), and glyceraldehyde-3-phosphate dehydrogenase (GAPDH) probe (nucleotide residues 22-553 for mouse GAPDH; GenBank accession number BC096440). Signals of bands on the blot were detected using a BAS-MS 2025 imaging plate (Fuji Photo Film, Tokyo, Japan) and visualized using a Typhoon 9400 scanner (GE Healthcare).

In vitro digestion analyses

Peptides were synthesized on an Applied Biosystems ABI 433A peptide synthesizer by using the standard fluorenylmethoxycarbonyl protocol, and purified by high-pressure liquid chromatography on a C-18 reverse-phase column. These peptides (2 pmol each) were incubated at 37°C for 30 hr in 25 mM Tris-HCl, pH 9.0, 2.5 μM $ZnCl_2$, and 0.005% Brij-35, with or without recombinant TACE (250 ng) in a final volume of 10 μl. After purification using pipette tips packed with a C18 resin (ZipTip, Millipore Corp.), the samples were analyzed by matrix-assisted laser desorption ionization-time of flight mass spectrometry (MALDI-TOFMS) (Reflex III, Bruker Daltonics) using α-cyano-4-hydroxycinnamic acid (CHCA) matrix (Sigma).

II.3 Results

Expression profile of Ptprz in the adult mouse brain.

It is well known that three splicing variants of Ptprz are expressed in the brain from a single gene (see Fig. II-1). All three isoforms expressed in the brain are highly glycosylated with chondroitin sulfate (CS) (Nishiwaki et al., 1998). Therefore, the removal of the chondroitin sulfate chains beforehand is necessary to resolve their core proteins by SDS-PAGE (Maeda et al., 1995).

When the chABC-treated extract of the wild-type mouse brain was analyzed with anti-Ptprz-S, which recognizes the extracellular region of all three isoforms (see Fig. II-1), six bands (bands *b* to *g*) in the range from 300 to 70 kDa were detected (Fig. II-2A). Because these bands are not present in *Ptprz*-deficient mice (-/-), all these molecular species are considered to be derived from *Ptprz* gene products. Among them, the 300-kDa (band *b*) and 250-kDa (band *c*) species represent the core proteins of Ptprz-S and Ptprz-B, respectively (Nishiwaki et al., 1998), however, the other four species (bands *d*-*g*) have not been characterized: The band of Ptprz-A (380 kDa) is scarcely detected (the position was indicated by "*a* with asterisk" in Fig. II-2; Shitani et al., 1998). The signal intensity of the three lower molecular species (bands *e*-*g*) was not changed by chABC treatment (Fig. II-2A), indicating that they are not modified with CS. In contrast, the larger bands *b*-*d* were almost missing without chABC-treatment, because they could not enter the gel.

To identify the receptor isoforms and their derivatives, the same blot was reprobed with anti-RPTPβ which recognizes the intracellular region (see Fig. II-1). As shown in Figure II-B, the 250-kDa species (band *c*, Ptprz-B) was detected by anti-RPTP□ as

expected, along with additional bands at around 75 kDa. The enlarged view of the 75-kDa band (lower panel), demonstrated that the signal consists of two adjacent bands of 77 kDa (band *h*) and 73 kDa (band *i*). On the other hand, anti-RPTPβ did not recognize the other species (bands *b*, *d, e-g*) detected by anti-Ptprz-S.

Although the uncharacterized species of Ptprz (bands *d-i*) appears to be processing products of the mature three isoforms of Ptprz, we addressed the possibility with the best of care that unknown novel *Ptprz* transcripts might be expressed by Northern blotting. Probe 1 for the CAH-FNIII region, which should detect all *Ptprz* transcripts, demonstrated that the three transcripts of 8.5 kb (*Ptprz-A*), 7.5 kb (*Ptprz-S*), and 5.8 kb (*Ptprz-B*) are expressed only in the wild-type, not in the knockout mice (Fig. II-3). Probe 2 for the PTP-D1 region, which detects the transcripts for the receptor isoforms, showed the 8.5-kb (*Ptprz-A*) and 5.8-kb (*Ptprz-B*) transcripts as expected. Although full-length Ptprz-A protein was hardly detected in the adult brain lysate, its mRNA was thus expressed in a significant amount. Importantly, other transcripts corresponding to the smaller Ptprz proteins such as the 180-kDa species or 75-kDa species were not detected.

Ectodomain shedding of Ptprz by metalloproteinases.

In my studies to exogenously express Ptprz-B in mammalian cells, I noticed that an immunoreactive species of 180 kDa (band *d* observed in the brain in Fig. II-2A) is present in the culture medium. Since this size corresponded to that of the whole extracellular region of Ptprz-B, I assumed that this is generated by the ectodomain shedding, a specialized type of limited proteolysis releasing the extracellular domain of a variety of cell surface receptors (Arribas and Borroto, 2002): It occurs in the vicinity

of the cell surface, generally dependent upon the actions of matrix metalloproteinases (MMPs) or adamalysins (ADAMs, a disintegrin and metalloproteinases).

I tested this possibility by using a PKC activator, phorbol 12-myristate 13-acetate (PMA), which is known to trigger ectodomain shedding in various cell types. The treatment of HEK293T cells expressing Ptprz-B with PMA resulted in an increase in the 180-kDa species in the conditioned medium in a dose-dependment manner, and which was inversely correlated with the decrease in Ptprz-B in cell extracts (Fig. II-4). This strongly suggests that the band of 180 kDa represents the ectodomain (Z_B-ECF) of Ptprz-B. Intriguingly, in the presence of a broad-spectrum metalloproteinase inhibitor, GM6001, the generation of the 180-kDa species was clearly inhibited under both un-stimulated and stimulated conditions with PMA (Fig. II-5).

Similar results were observed with the Ptprz-A isoform. Unlike Ptprz-B, when Ptprz-A was expressed in HEK293T cells, the mature receptor protein was highly modified with CS (data not shown). Therefore, the samples were treated with chABC before SDS-PAGE. As with Ptprz-B, the release of the extracellular fragment, Z_A-ECF of 300 kDa into the culture medium was clearly enhanced by PMA, and suppressed in the presence of GM6001 (Fig. II-6). On the other hand, when the secretory isoform (Ptprz-S) was expressed, the full-length Ptprz-S was detected exclusively in the medium, and the amount was not affected by the treatment of cells either with PMA or with GM6001 (Fig. II-6). It is recognizable here that Z_A-ECF is indistinguishable from Ptprz-S in size and antigenicity.

TACE-mediated shedding of Ptprz.

Because GM6001 is a broad-spectrum metalloproteinase inhibitor, additional

experiments were required to define the specific proteinase(s) involved in the ectodomain shedding of Ptprz-A and -B. Tumor necrosis factor-α (TNF-α) converting enzyme (TACE, also known as ADAM-17) is a GM6001-sensitive, membrane-anchored, Zn-dependent metalloproteinase. TACE functions as a membrane sheddase to release the ectodomain portions of many transmembrane proteins including TNF-α and Notch (Blobel, 2002). To determine whether TACE is involved in the ectodomain cleavage of Ptprz, I took advantage of CHO-M2 cells which are defective in TACE-mediated shedding (Borroto et al., 2003). Parental wild-type CHO cells (CHO-WT) and CHO-M2 cells which stably express a functional TACE, CHO-(M2+TACE), were also used for comparison.

Transfection of the expression construct of Ptprz-B yielded similar expression levels of Ptprz-B in these cells (Fig. II-7, left panels), and similar amounts of Z_B-ECF were accumulated in the conditioned media during 1 hr of incubation (Fig. II-7, right panels): This basal level of accumulation of Z_B-ECF was observed also in CHO-M2 and similarly suppressed by GM6001, indicating that the basal small amount of ectodomain shedding of Ptprz-B is independent of TACE. However, PMA stimulated ectodomain cleavage in CHO-WT and CHO-(M2+TACE) cells but not in CHO-M2 cells. The inhibition of PMA-enhanced shedding by GM6001 was reproduced in both CHO-WT and CHO-(M2+TACE) cells. Similar results were observed with Ptprz-A. TACE is thus highly responsible for the PMA-inducible cleavage of Ptprz for the generation of Z_B-ECF and Z_A-ECF, but not for the constitutive cleavage in these cell lines.

Since the Ptprz-A and Ptprz-B isoforms have a common short sequence in the extracellular membrane-proximal region, the cleavage site was expected within this

region. When a synthetic peptide corresponding to the juxtamembrane sequence was incubated with recombinant TACE *in vitro*, TACE did induce the cleavage of the substrate peptide into the two fragments (Fig. II-8B). The molecular mass of them indicated that the enzymatic cleavage occurs between Gly at 1631 (P1 site) and Leu at 1632 (P1' site) (Fig. II-8A). Previous studies with peptide substrates of TNF-α indicated that TACE has a strong preference for cleavage at Ala-Val sequences, and cannot cleave a TNF-α-based peptide with the substitution of Ala with Ile at the P1 position (Jin et al., 2002). Consistently, a mutant peptide, Zejm(G/I), in which Gly at P1 is replaced with Ile, was hardly cleaved by TACE (Fig. II-8C). In contrast, the cleavage was highly enhanced by substitution with Ala at P1, Zejm (G/A), the same as TNF-α (Fig. II-8D)

I confirmed the validity of this *in vitro* result by generating the mutant construct of Ptprz-B and expressing it in CHO-WT and CHO-M2 cells. Changing Gly at 1631 to Ile (G1631I) did not affect the efficiency of the basal constitutive ectodomain cleavage, however, the efficiency of the ectodomain cleavage enhanced by PMA was markedly decreased in the G1631I-mutant of Ptprz-B (Fig. II-8E). In TACE-defective CHO-M2 cells, both wild-type Ptprz-B and the G1631I mutant showed a similar accumulation of Z_B-ECF with and without PMA stimulation, indicating that TACE indeed cleaves the Gly-Leu bond in CHO cells (Fig. II-8E).

TACE-independent basal (constitutive) shedding was not affected by the G1631I-mutation (Fig. II-8E), suggesting that there exist multiple cleavage sites within the membrane proximal region by different ADAMs or MMPs other than TACE. In line with this view, I found that recombinant MMP-9 can cleave the peptide substrate Zejm(wild) at two sites, between Arg (1625) - Ile (1626) and Gly (1627) - Leu (1628),

located in the vicinity of the TACE cleavage site (Fig. II-9). I confirmed that the peptide cleavage by MMP-9 is not affected by substitution of either Gly to Ile (Fig. II-9E and II-9F) or Gly to Ala (Fig. II-9G and II-9H). The ectodomain shedding thus occurs within the common membrane proximal region in the two receptor isoforms in both a constitutive and a PMA-stimulated manner.

Metalloproteinase-mediated proteolytic cleavage of Ptprz in vivo.

To verify the occurrence of the metalloproteinase-mediated cleavage of Ptprz *in vivo*, mice were administered with GM6001 as described in a recent study (Wang et al., 2005). As all three Ptprz isoforms are expressed in the brain, we thought that it might be difficult to discriminate the proteolytic products. I therefore tested the effect of GM6001 in the eye ball first, because where Ptprz-B is exclusively expressed (data not shown). When the extract prepared from the eyeball was analyzed, the signal intensity of the 180-kDa species (Z_B-ECF) was found to be markedly decreased as compared with that of Ptprz-B (250 kDa) at 48 hr by single administration of GM6001 (Fig. II-10A). This indicates that metalloproteinase-mediated processing of Ptprz occurs under physiological conditions. The decrease in the relative amount of Z_B-ECF to Ptprz-B was reproduced in the brain by continuous intraventricular infusion of GM6001 for 4 days (Fig. II-10B).

Regulated intracellular processing of Ptprz.

In most cases, membrane-associated fragments that are generated by metalloproteinase-mediated cleavage of transmembrane proteins are converted to cytosolic fragments by regulated intramembrane proteolysis (RIP) with an active

γ-secretase complex (Selkoe and Kopan, 2003). In the extracts of HEK293T cells expressing Ptprz-B, the 73-kDa band was observed with anti-RPTPβ (Fig. II-2). To determine whether the 73-kDa band represents either the membrane-tethered fragment ZΔE or the intracellular fragment Z-ICF (see Fig. II-11A), cells were treated with a γ-secretase inhibitor, compound E, which was expected to induce the accumulation of ZΔE by suppressing the conversion of ZΔE to Z-ICF. In the presence of compound E, the signal intensity of the 73-kDa band was increased in both vehicle-stimulated and PMA-stimulated conditions (Fig. II-11A). On the other hand, upon treatment with a proteasome inhibitor, lactacystin, which is expected to inhibit the degradation of Z-ICF, the signal intensity of the 73-kDa band was again increased in PMA-stimulated cells (Fig. II-11A). These results indicate that the band of ZΔE overlaps with that of Z-ICF, and that Z-ICF produced from ZΔE by RIP is probably degraded by the proteasome under normal conditions.

For discrimination between ZΔE and Z-ICF, I conducted immunofluorescent staining of cells to characterize their subcellular localization. As shown in Figure II-11B, in the basal condition, anti-RPTPβ immunoreactivity was exclusively localized to the cell surface in Ptprz-B-positive cells, whereas the cell surface signal was considerably decreased by PMA treatment along with a slight increase in the intracellular staining. In the presence of compound E to inhibit γ-secretase cleavage, PMA-induced decrease in the cell surface signal was apparently prevented, indicating that the cell membrane-tethered ZΔE occupies the majority of the 73-kDa species in this condition. In contrast, when cells were stimulated with PMA in the presence of lactacystin to inhibit proteasomal degradation, the immunoreactivity was mainly localized to the intracellular compartment, and furthermore, several immunoreactive

puncta were observed in the nucleus. Therefore, in this condition, the intracellular fragment Z-ICF is substantially accumulated in the cell, while some amounts of Ptprz-B and ZΔE remain on the cell surface. A similar distribution was observed when the entire intracellular region of Ptprz (PtprzICR) was expressed using a cDNA construct, where the signal in the nucleus was more evident. There was no signal of PtprzICR at the cell membrane, indicating that the intracellular domain of Ptprz cleaved by γ-secretase is not tethered to the membrane anymore.

To verify that the generation of Z-ICF is dependent on the activity of presenilin (PS), the catalytic subunit of the γ-secretase, Ptprz-B was transiently expressed in HEK293 cells stably expressing wild-type PS1 or a dominant negative mutant, PS1 D385A (Kasuga et al., 2007). In the presence of lactacystin, PMA-enhanced intracellular staining was markedly enhanced in cells expressing wild-type PS1, but not in cells expressing PS1 D385A (Fig. II-11C). This indicates that the generation of Z-ICF is dependent on the PS activity.

II.4 Discussion

In the present study, I demonstrated by cell-based assays that the two receptor isoforms of Ptprz, Ptprz-A and Ptprz-B, undergo metalloproteinase-mediated ectodomain shedding, which releases the extracellular fragment, $Z_{A/B}$-ECF, from the cell surface, and produces the membrane-tethered counterpart ZΔE. Importantly, administration of GM6001 to mice demonstrated its physiological occurrence. ZΔE is subsequently digested by PS/γ-secretase, and the cytoplasmic fragment (Z-ICF) is released from the plasma membrane to not only the cytoplasm but also the nucleus, suggesting a novel signaling pathway of Ptprz. I summarized their molecular natures (Fig. II-13A), and corresponding bands observed in the brain (Fig. II-13B). I have not included the identification of lower molecular species (bands *e*-*g*) observed in the brain to avoid confusion; however, I have already revealed that they are produced by the proteolytic cleavage of the extracellular region of Ptprz-A/B and Ptprz-S by plasmin (see Chapter 3). I have also identified that the upper species (77 kDa, band *h*) of the doublet bands is produced by proteolytic cleavage of exon 16 (a cytoplasmic exon)-deleted form of Ptprz-A/B (data not shown).

Several groups (Maurel et al., 1994; Canoll et al., 1996) including ours have reported that three transcripts corresponding to *Ptprz-A*, *Ptprz-B*, and *Ptprz-S* are expressed in the adult brain. On the other hand, a cDNA clone for phosphacan short isoform (PSI), an isoform of Ptprz which roughly corresponds to the extracellular fragment of Ptprz-B, was reported recently from a neonatal mouse brain cDNA library (Garwood et al., 2003). However, I could not detect the corresponding transcript of 4 kb for PSI in the adult mouse brain (Fig. II-3). Moreover, I could not find out the sequence corresponding to the 3'-UTR of PSI (GenBank accession number AJ428208)

in or near the mouse *Ptprz* gene (the Ensembl database, http://www.ensembl.org/; release 48 - Dec 2007). I suspect that the PSI cDNA clone is a cloning artifact obtained by ligation with an unrelated cDNA fragment. In addition, I did not find any evidence for the presence of *PTPRZ2*, which was reported as a familial gene on human chromosome 1 at p36 (Onyango et al., 1998), by searching databases of the human and mouse genomes.

The core protein of Ptprz-A has been hardly detected in the adult brain (Fig. II-2) as described (Nishiwaki et al., 1998), in spite of the significant expression at the mRNA level (Fig. II-3; Maurel et al., 1994; Canoll et al., 1996). This strongly suggests that almost all Ptprz-A is constitutively processed in the brain. Prototypically released Z_A-ECF has almost the same structure as Ptprz-S. Ptprz-S (phosphacan/6B4 proteoglycan) has been considered as the sole component of phosphate-buffered saline (PBS)-soluble chondroitin sulfate proteoglycan with a 300-kDa core protein in the brain (Maeda et al., 1994). However, densitometric analyses of the Western (Fig. II-2) and Northern (Fig. II-3) blots suggested that Z_A-ECF thus released may account for approximately one third of the total amount of phosphacan/6B4 proteoglycan.

The data obtained from TACE-defective CHO-M2 cells clearly showed that the PMA-stimulated shedding of the Ptprz receptor isoforms is mediated in part by TACE. Although release of the extracellular domains by metalloproteinase-mediated processing has been observed for several transmembrane proteins, the mechanism by which MMPs or ADAMs recognize and cleave the substrates is not well defined (Arribas and Borroto, 2002). The peptide digestion experiments *in vitro* identified the site of Ptprz's cleavage by TACE as between Gly (1631) and Leu (1632) (Fig II-8), corresponding to between the 6th and 7th residues outside the transmembrane domain of Ptprz-A/B.

This is consistent with the finding that the cleavage site in a variety of substrates is located within the ectodomain stalk region, at residues 2-20 from the transmembrane region. The mutation of Gly at position 1631 to Ile suppressed the TACE-mediated cleavage of Ptprz both *in vivo* and *in vitro*, whereas TACE-independent basal (constitutive) shedding was not affected thereby. I presume that there exist multiple cleavage sites within the membrane proximal region, which is common to the two receptor isoforms, by metalloproteinases(Fig. II-9).

One conspicuous defect in adult *Ptprz*-deficient mice is a significant enhancement of long-term potentiation (LTP) in the CA1 region of the hippocampus (Nissato et al., 2005) and learning deficits (Tamura et al., 2006). LTP is a long lasting augmentation of synaptic strength that has been suggested as a cellular mechanism underlying learning and memory. Our group recently reported that the tyrosine phosphorylation level of a GTPase-activating protein (GAP) for Rho GTPase, p190 RhoGAP, a substrate molecule of Ptprz, is decreased 1 hr after the conditioning in the hippocampus of wild-type mice, but not of *Ptprz*-deficient mice (Tamura et al., 2006), suggesting that the PTP activity of Ptprz may be up-regulated during learning. Dimerization-induced inactivation of RPTPs is a well known mechanism. Ligand binding to the extracellular region induces the dimerization (or oligomerization) of Ptprz and thereby inhibits the PTP activity (Fukada et al., 2006). The removal of the extracellular region by metalloproteinase-mediated processing presumably abolishes this ligand-induced inactivation mechanism. Of note is that the intracellular region of Ptprz (PtprzICR) efficiently dephosphorylates substrates in cultured cells (data not shown).

LTP exhibits two distinct phases (Reymann and Frey, 2007). The initial early phase (E-LTP), which is rapidly induced, only lasts ~1-2 h. This form does not require

protein synthesis, and reflects at least in part posttranslational modifications including phosphorylation and translocation of the synaptic proteins. The second, more slowly emerging late-phase (L-LTP), lasts many hours to days or longer. Interestingly, the MMP-9 protein level and accordingly the proteolytic activity are rapidly increased by stimuli that induce L-LTP in the CA1, and the pharmacological blockade of MMP-9 prevents the induction of L-LTP (Nagy et al., 2006). Thus, there is a possibility that Ptprz-B is a target of the MMP(s) associated with L-LTP. Ptprz receptor isoforms interact with the PSD95 family including PSD95, SAP97, and SAP102 through the carboxyl-terminal PDZ-binding motif (Kawachi et al., 1999; Fukada et al., 2005). In this context, TACE is also interesting, since this sheddase harbors a PDZ-binding motif at the C-terminus, and thereby associates with members of the PSD95 family (Peiretti et al., 2003). Notably, the C-terminal counterparts of Ptprz receptor isoforms (ZΔE or Z-ICF) are enriched in the postsynaptic density (PSD) fraction of the adult mouse brain (data not shown).

Ptprz may be thus implicated in L-LTP through the regulation of gene expression by regulated shedding, in addition to the simple dephosphorylation of the substrate molecules including p190 RhoGAP (Tamura et al., 2006) for E-LTP at central synapses. Our cell-based assays indicated that the intracellular fragment of Ptprz (Z-ICF) is translocated into the nucleus in cultured cells (Fig. II-11). Interestingly, overexpression of Z-ICF by pZeoSV-PtprzICR in glioblastoma cells stimulates the morphological differentiation (data not shown). Elucidating the functional roles of Z-ICF in the nucleus will be highly challenging themes. To determine whether the shedding of Ptprz by these processing enzymes is indeed involved in the formation of LTP remains as future studies.

Fig. II-1. Schematic representation of Ptprz isoforms. Molecular sizes of the chondroitin sulfate proteoglycan forms (CS-PG) and their core proteins after treatment with chondroitinase ABC (chABC) are shown. Regions corresponding to the epitopes of antibodies used in this study are indicated by vertical bars. Domains are highlighted in different colors: CAH, carbonic anhydrase-like domain; FNIII, fibronectin type III domain; PTP-D1 and PTP-D2, tyrosine phosphatase domains.

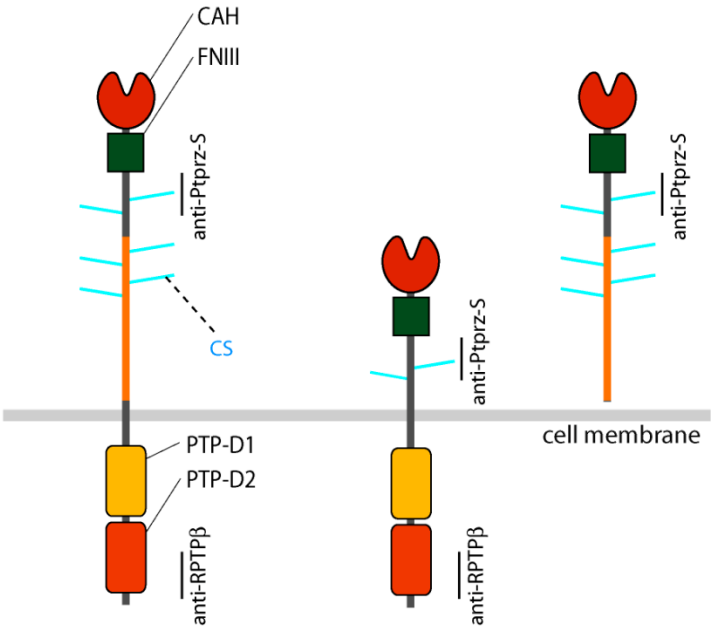

	Ptprz-A	Ptprz-B	Ptprz-S
core protein (kDa)	380	250	300
CS-PG form (kDa)	600 -1000	400	600 -1000

Fig. II-2. Novel protein species of Ptprz in the adult mouse brain. A-C, Brain extract (5 μg protein) of wild-type mice (+/+) and *Ptprz*-deficient mice (-/-) was treated with (+) or without (-) chABC. The samples were separated on a 5-20% gradient gel, followed by Western blotting using anti-Ptprz-S (A). The same blot was stripped, and reprobed with anti-RPTPβ (B). The lower image is a vertical enlargement of the area enclosed by a rectangle in the upper image. Staining with coomassie brilliant blue R-250 to check the amounts of protein applied (C).

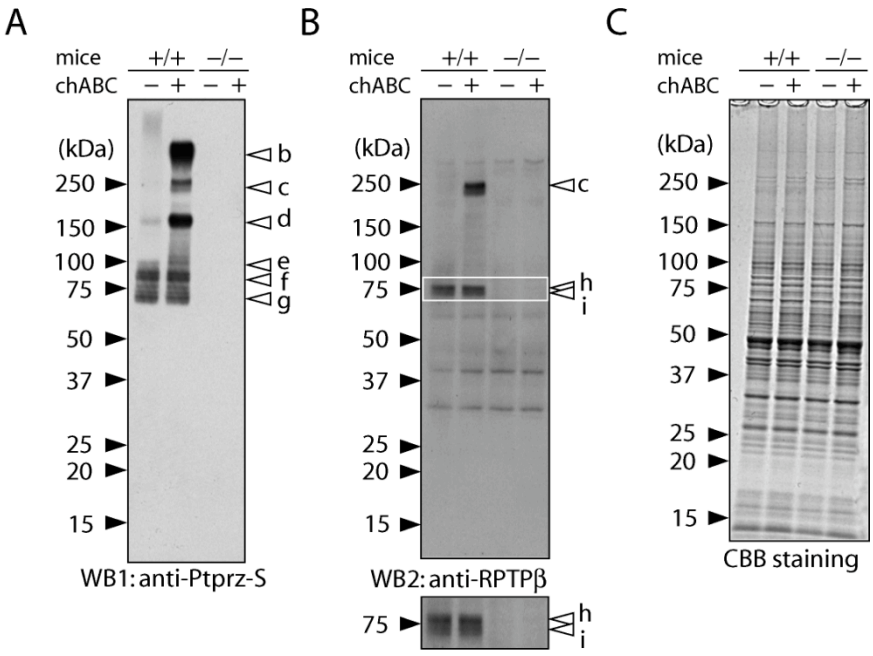
A
mice
+/+
−/−
chABC
− + − +
(kDa)
250
150
100
75
50
37
25
20
15
b
c
d
e
f
g
WB1: anti-Ptprz-S
B
mice
+/+
−/−
chABC
− + − +
(kDa)
250
150
100
75
50
37
25
20
15
c
h
i
WB2: anti-RPTPβ
75
h
i
C
mice
+/+
−/−
chABC
− + − +
(kDa)
250
150
100
75
50
37
25
20
15
CBB staining

Fig. II-3. Northern blot analyses of *Ptprz* transcripts in the adult mouse brain. Poly(A)$^+$ RNA (2 μg) from the adult mouse brain was hybridized with a ^{32}P-labeled cDNA probe for the CAH-FNIII region (probe 1). The same blot was stripped, and then reprobed for the PTP-D1 region (probe 2). The amount of RNA loaded was confirmed with a probe for glyceraldehyde-3-phosphate dehydrogenase (GAPDH) in the same blot.

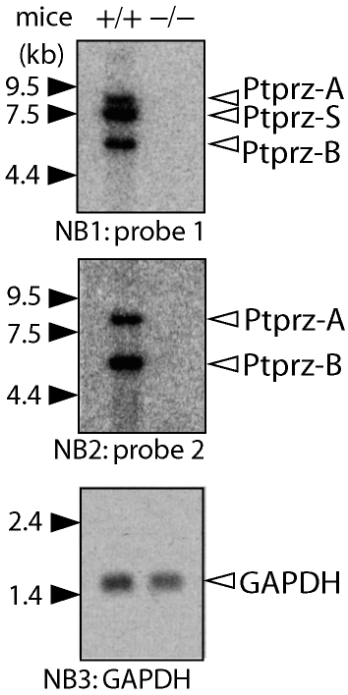
mice +/+ −/−
(kb)
9.5
7.5
4.4
Ptprz-A
Ptprz-S
Ptprz-B
NB1: probe 1
9.5
7.5
4.4
Ptprz-A
Ptprz-B
NB2: probe 2
2.4
1.4
GAPDH
NB3: GAPDH

Fig, II-4. PMA-induced ectodomain shedding of Ptprz-B in a dose-dependent manner. HEK293T cells were transiently transfected with the expression construct of Ptprz-B or control vector (Moc). Twenty-four hours after transfection, cells were washed and incubated with indicated amount of PMA in fresh serum-free medium for 1 hr. The cell extracts (left panels) and conditioned media (right panel) were analyzed by Western blotting using anti-Ptprz-S.

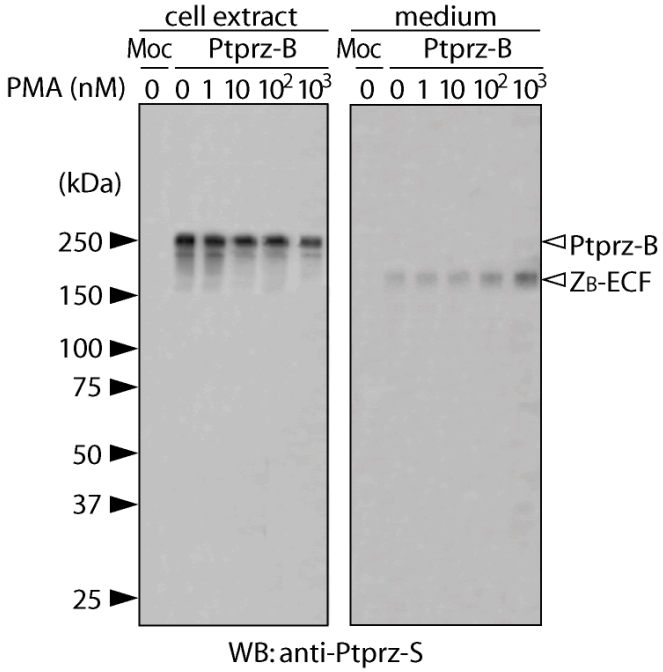
cell extract
medium
Moc
Ptprz-B
Moc
Ptprz-B
PMA (nM)
0 0 1 10 10² 10³
0 0 1 10 10² 10³
(kDa)
250
150
100
75
50
37
25
Ptprz-B
ZB-ECF
WB: anti-Ptprz-S

Fig. II-5. Metalloproteinase-mediated ectodomain cleavage of the receptor isoforms of Ptprz-B. HEK293T cells were transiently transfected with the expression construct of Ptprz-B or control vector (Moc). Twenty-four hours after transfection, cells were washed and incubated with or without PMA in fresh serum-free medium for 1 hr. GM6001 was added 20 min prior to the stimulation by PMA or vehicle. The cell extracts (left panels) were analyzed by Western blotting using anti-Ptprz-S. The same membrane was then reprobed with anti-RPTPβ. Conditioned media (right panel) were analyzed with anti-Ptprz-S. The designations are shown in Fig. II-13.

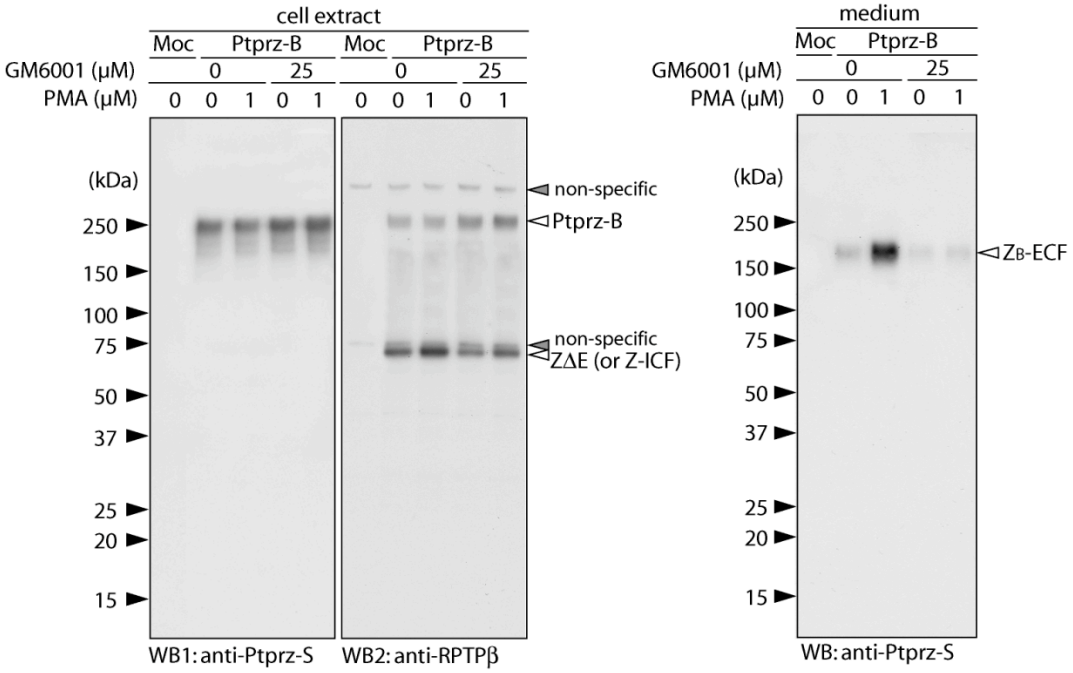
cell extract
Moc
Ptprz-B
Moc
Ptprz-B
GM6001 (μM)
0
25
0
25
PMA (μM)
0 0 1 0 1 0 0 1 0 1
(kDa)
250
150
100
75
50
37
25
20
15
non-specific
Ptprz-B
non-specific
ZΔE (or Z-ICF)
WB1: anti-Ptprz-S
WB2: anti-RPTPβ
medium
Moc
Ptprz-B
GM6001 (μM)
0
25
PMA (μM)
0 0 1 0 1
(kDa)
250
150
100
75
50
37
25
20
15
ZB-ECF
WB: anti-Ptprz-S

Fig. II-6. Metalloproteinase-mediated ectodomain cleavage of the receptor isoforms of Ptprz-A. HEK293T cells were transiently transfected with the expression construct of Ptprz-A, Ptprz-S or control vector (Moc). Twenty-four hours after transfection, cells were washed and incubated with or without PMA in fresh serum-free medium for 1 hr. GM6001 was added 20 min prior to the stimulation by PMA or vehicle. The cell extracts (left panels) were analyzed by Western blotting using anti-Ptprz-S. Conditioned media (right panel) were analyzed with anti-Ptprz-S. The designations are shown in Fig. II-13.

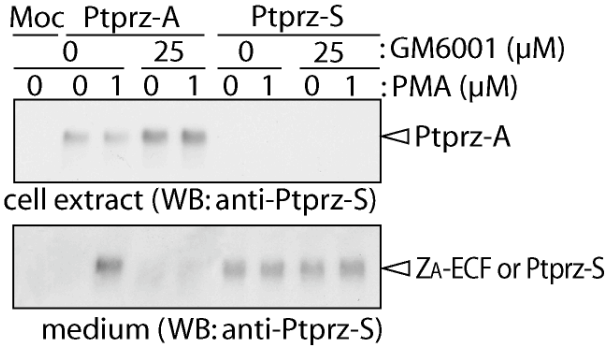
Moc
Ptprz-A
Ptprz-S
0
25
0
25
: GM6001 (μM)
0 0 1 0 1 0 1 0 1
: PMA (μM)
Ptprz-A
cell extract (WB: anti-Ptprz-S)
ZA-ECF or Ptprz-S
medium (WB: anti-Ptprz-S)

Fig. II-7. Involvement of TACE in PMA-stimulated ectodomain cleavage of Ptprz. CHO-WT (wild type), CHO-M2 (TACE defective) and CHO-(M2+TACE) (M2 cells expressing functional TACE) cells were transiently transfected with the Ptprz-B expression construct. Twenty-four hours after transfection, cells were washed and incubated in fresh serum-free medium with or without PMA for 1 hr. GM6001 was added 20 min prior to PMA or vehicle. The cell extracts (left panels) and conditioned media (right panels) were analyzed by Western blotting with anti-Ptprz-S. The arrows with asterisks indicate immature forms of Ptprz-B accumulated in cells. The designations are shown in Fig. II-13.

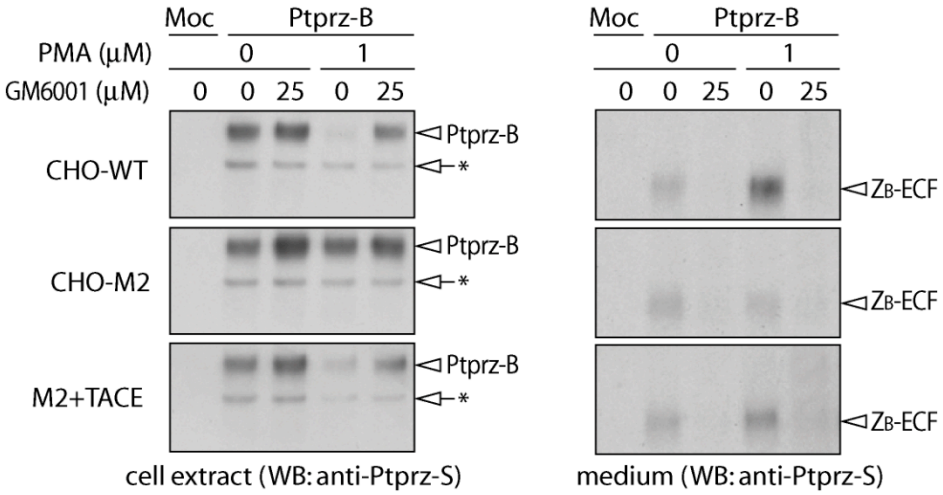
Moc
Ptprz-B
PMA (μM)
0
1
GM6001 (μM)
0 0 25 0 25
CHO-WT
CHO-M2
M2+TACE
Ptprz-B
*
ZB-ECF
cell extract (WB: anti-Ptprz-S)
medium (WB: anti-Ptprz-S)

Fig. II-8. Identification of the TACE-cleavage site in Ptprz. A, Amino acid sequence of the common extracellular membrane-proximal region in Ptprz-A and Ptprz-B. Amino acid numbers refer to the sequence of rat Ptprz-A. Three synthetic peptides are shown under the sequence. The arrowhead indicates the TACE cleavage site deduced by *in vitro* peptide digestion as below. TM, transmembrane segment. B-D, Synthetic peptides only (left panels) or synthetic peptides with recombinant TACE (right panels) were incubated for 30 hr at 37°C, and the products were analyzed by mass spectrometry (see Materials and Methods). The combination of peptides is shown at the top left corner of each panel. Peaks are labeled with arrowheads as in A. The expected *m*/*z* value for the N-terminal fragment when cleaved at the Ile-Leu bond of Zejm(G/I) is indicated by an open arrow (C, right panel). E, CHO-WT and CHO-M2 were transiently transfected with expression constructs for wild-type or G1631I mutant of Ptprz-B. Twenty-four hours after transfection, cells were washed and incubated in fresh serum-free medium with or without PMA for 1 hr. The cell extracts (upper panel) and conditioned media (lower panel) were analyzed by Western blotting with anti-Ptprz-S. The designations are shown in Fig II-13.

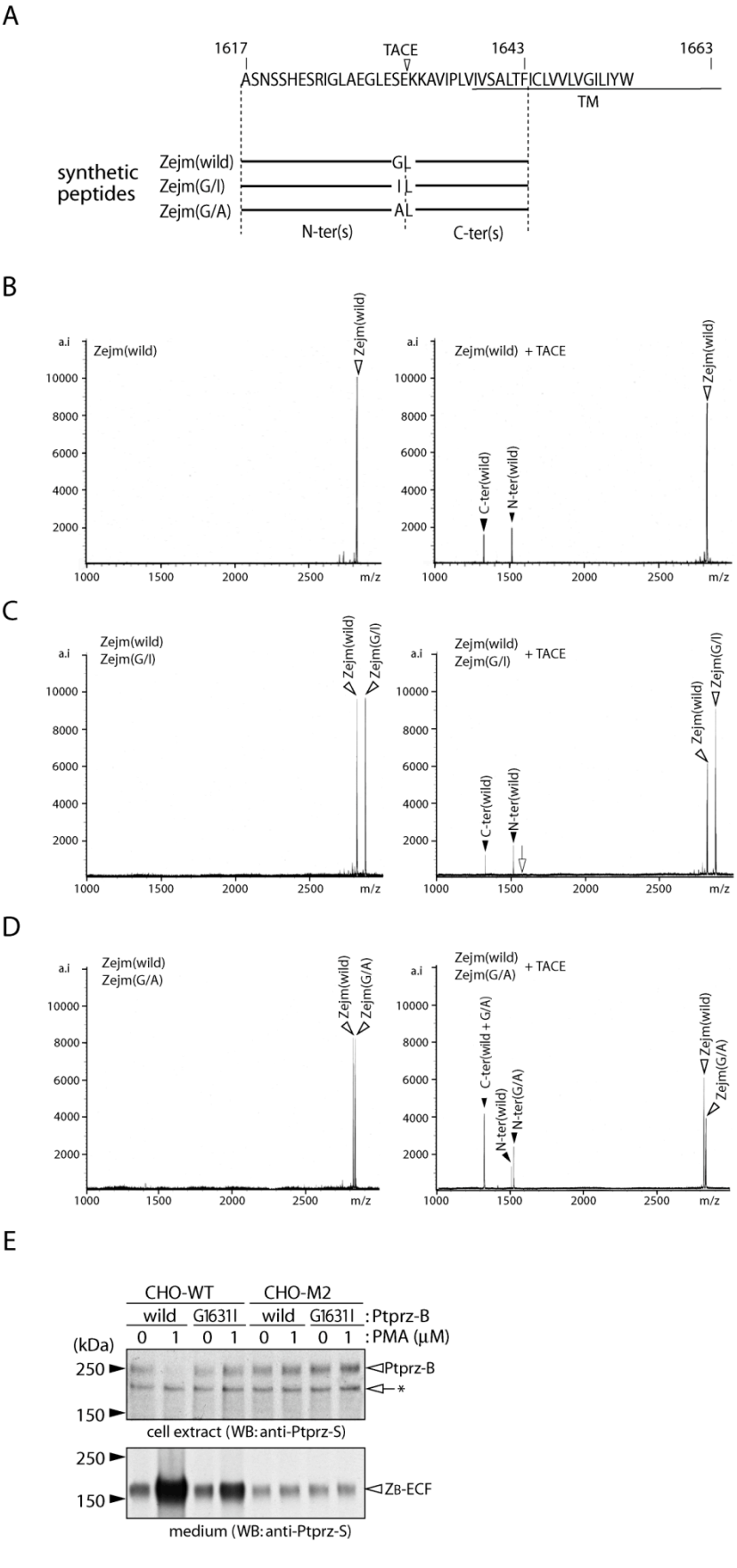
A
1617
TACE
1643
1663
ASNSSHESRIGLAEGLESEKKAVIPLVIVSALTFICLVVLVGILIYW
TM
synthetic peptides
Zejm(wild)
Zejm(G/I)
Zejm(G/A)
GL
IL
AL
N-ter(s)
C-ter(s)
B
Zejm(wild)
Zejm(wild) + TACE
C-ter(wild)
N-ter(wild)
C
Zejm(wild)
Zejm(G/I)
Zejm(wild)
Zejm(G/I) + TACE
D
Zejm(wild)
Zejm(G/A)
Zejm(wild)
Zejm(G/A) + TACE
C-ter(wild + G/A)
N-ter(G/A)
a.i
m/z
E
CHO-WT
CHO-M2
wild
G1631I
: Ptprz-B
: PMA (μM)
(kDa)
250
150
Ptprz-B
*
cell extract (WB: anti-Ptprz-S)
ZB-ECF
medium (WB: anti-Ptprz-S)

Fig. II-9 *In vitro* cleavage of Ptprz by MMP-9**.** A, The amino acid sequence of the extracellular membrane-proximal region common to Ptprz-A and Ptprz-B, and synthetic peptides used are shown below. Arrowheads indicate the MMP-9 cleavage site deduced by *in vitro* peptide digestion with MMP-9 as below. B-H, Samples were incubated in 10 μl of 50 mM Tris-HCl, pH 7.6, 150 mM NaCl, 5 mM $CaCl_2$, and 0.01% Brij-35 for 6 hr at 37 °C (2 pmol, each peptide; 0.1 μg recombinant MMP-9, Calbiochem), and then analyzed by mass spectrometry. The combination of peptide and/or MMP-9 is shown at the top left corner of each panel. Peaks are labeled as in A. MMP-9 can cleave the Zejm peptides at two sites; Arg (1625) - Ile (1626) and Gly (1627) - Leu (1628) of Ptprz-A.

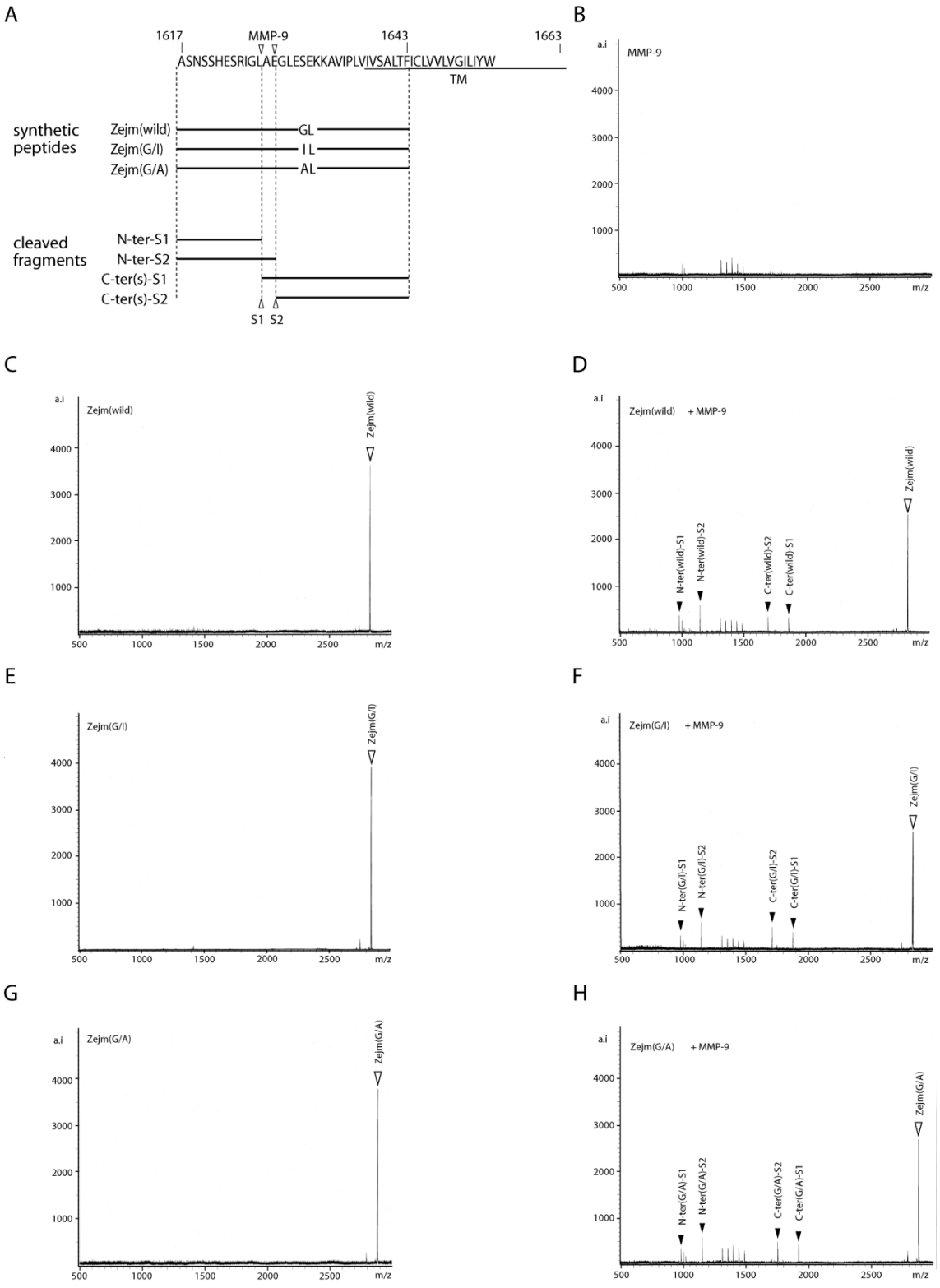
A
1617
MMP-9
1643
1663
ASNSSHESRIGLAEGLESEKKAVIPLVIVSALTFICLVVLVGILIYW
TM
synthetic peptides
Zejm(wild)
Zejm(G/I)
Zejm(G/A)
GL
I L
AL
cleaved fragments
N-ter-S1
N-ter-S2
C-ter(s)-S1
C-ter(s)-S2
S1 S2
B
MMP-9
C
Zejm(wild)
D
Zejm(wild) + MMP-9
N-ter(wild)-S1
N-ter(wild)-S2
C-ter(wild)-S2
C-ter(wild)-S1
E
Zejm(G/I)
F
Zejm(G/I) + MMP-9
N-ter(G/I)-S1
N-ter(G/I)-S2
C-ter(G/I)-S2
C-ter(G/I)-S1
G
Zejm(G/A)
H
Zejm(G/A) + MMP-9
N-ter(G/A)-S1
N-ter(G/A)-S2
C-ter(G/A)-S2
C-ter(G/A)-S1
a.i
m/z

Fig. II-10. Metalloproteinase-mediated cleavage of Ptprz *in vivo*. A, Tissue extracts of eye balls were prepared from wild-type mice 48 hr after administration of GM6001 or vehicle (con). The extracts (5 μg protein) were treated with chABC and then analyzed by Western blotting using anti-Ptprz-S. Densitometric analysis indicated a significant decrease in the amount of Z_B-ECF relative to that of Ptprz-B in mice treated with GM6001 as compared to those treated with vehicle (n = 4, each group). Values are expressed as the mean ± SEM. *$p < 0.05$; Student's t-test (n=4) (right graph). B, Wild-type mice were received a continuous intracerebroventricular infusion of GM6001 or vehicle (con) for 4 days. Tissue extracts of the midbrain region (corresponding to the midbrain, thalamus, and subthalamus) were analyzed as above. There was a significant decrease in the amount of Z_B-ECF relative to that of Ptprz-B in mice treated with GM6001 as compared to those treated with vehicle (con) treatments (Student's t-test, n = 3 each). Values are expressed as the mean ± SEM. The designations are shown in Fig II-13.

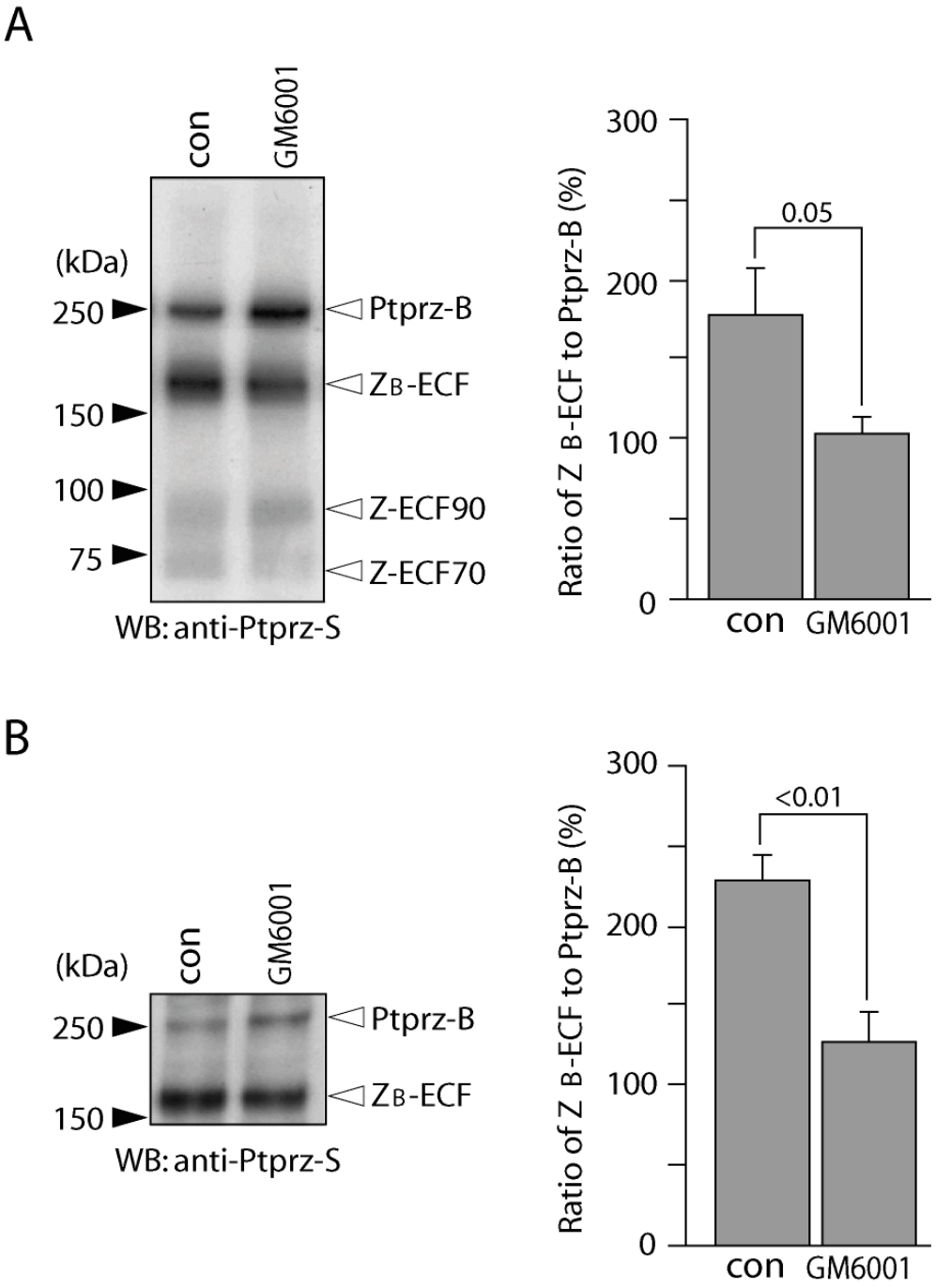
A
con
GM6001
(kDa)
250
150
100
75
Ptprz-B
ZB-ECF
Z-ECF90
Z-ECF70
WB: anti-Ptprz-S
Ratio of Z B-ECF to Ptprz-B (%)
300
200
100
0
0.05
con
GM6001
B
con
GM6001
(kDa)
250
150
Ptprz-B
ZB-ECF
WB: anti-Ptprz-S
Ratio of Z B-ECF to Ptprz-B (%)
300
200
100
0
<0.01
con
GM6001

Fig. II-11. Presenilin/γ-secretase-mediated intramembrane cleavage of Ptprz. A, HEK293T cells expressing Ptprz-B were pretreated with vehicle, compound E (1 μM), or lactacystin (5 μM) for 3 hr, then cultured with or without PMA stimulation for 1 hr. Cell extracts were analyzed by Western blotting using anti-RPTPβ. The designations are shown in Fig. II-13. B, HEK293T cells treated as described in A were immediately fixed with formalin, and stained with anti-RPTPβ. In addition, HEK293T cells that were transiently transfected with the expression construct of the entire intracellular region of Ptprz (PtprzICR) were also analyzed as above. The fluorescence images of anti-RPTPβ staining (green) and merged images with TOPRO-3-stained nuclei or with differential interference contrast (DIC) images are shown. The rightmost images are enlargements of the area enclosed by a square in the adjacent images. Scale bars, 10 μm.

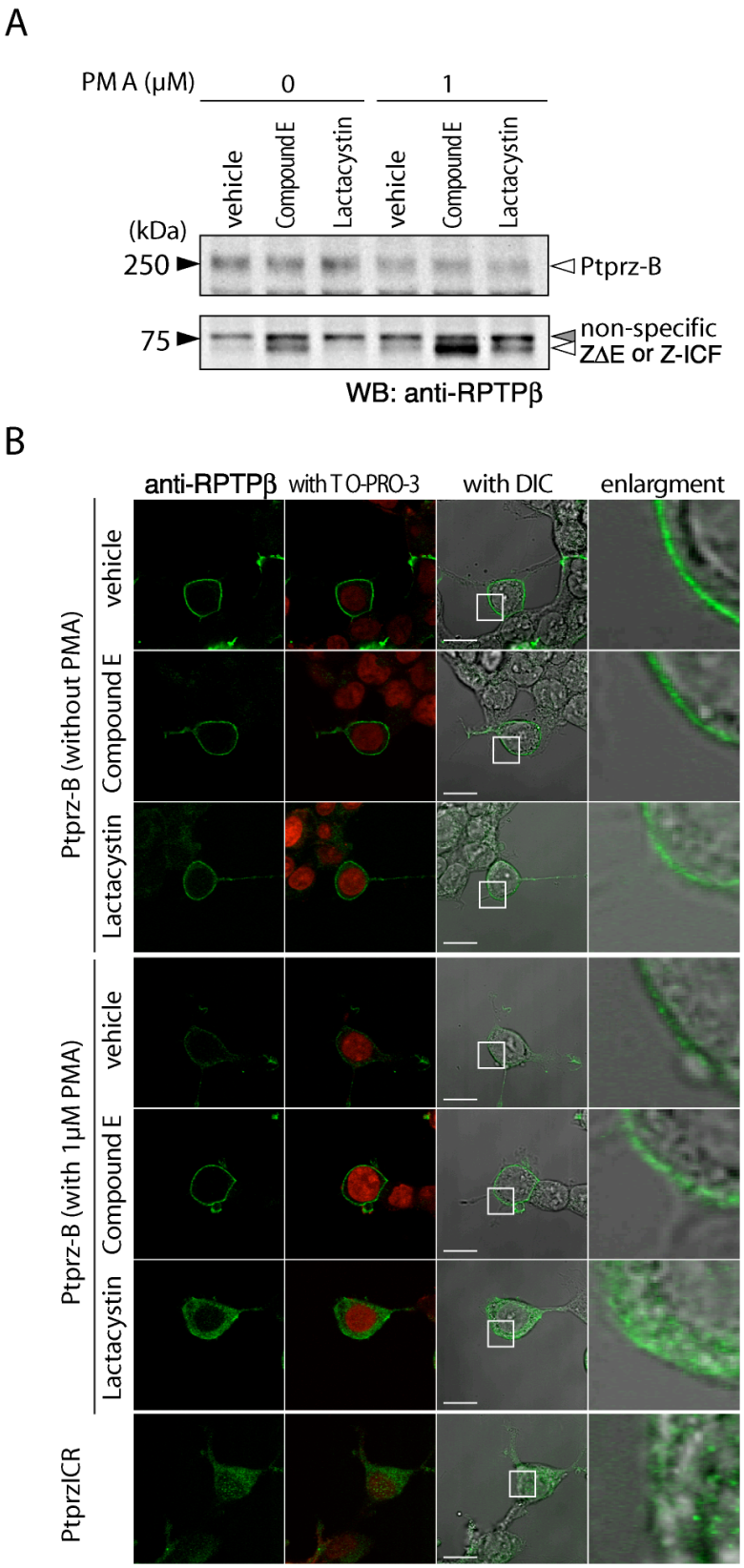
A
PM A (μM)
0
1
vehicle
Compound E
Lactacystin
vehicle
Compound E
Lactacystin
(kDa)
250
Ptprz-B
75
non-specific
ZΔE or Z-ICF
WB: anti-RPTPβ
B
anti-RPTPβ
with TO-PRO-3
with DIC
enlargment
Ptprz-B (without PMA)
vehicle
Compound E
Lactacystin
Ptprz-B (with 1μM PMA)
vehicle
Compound E
Lactacystin
PtprzICR

Fig. II-12. Intramembrane cleavage of Ptprz in HEK cells stably expressing presenilin or its dominant-negative variant. A, HEK293 cells stably expressing either wild-type presenilin 1 (PS1WT) or a dominant-negative PS1 variant (PS1D385A) were transiently transfected with the Ptprz-B expression construct. Twenty-four hours after transfection, cells were treated and analyzed by Western blotting using anti-RPTPβ as described in Fig. II-11. The designations are shown in Fig II-13. B, The cells treated as described in *A* were fixed, and stained with anti-RPTPβ (green). Merged images with TO-PRO-3-stained nuclei (red) and differential interference contrast images (DIC) are also shown. Scale bars, 10 μm. The figures are representative of three separate experiments.

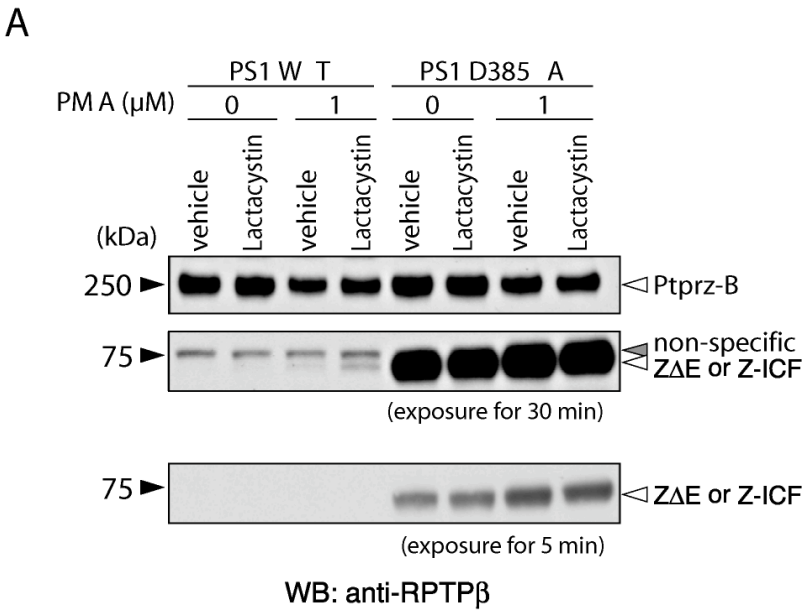
A
PS1 W T
PS1 D385 A
PM A (μM)
0
1
0
1
vehicle
Lactacystin
vehicle
Lactacystin
vehicle
Lactacystin
vehicle
Lactacystin
(kDa)
250
Ptprz-B
75
non-specific
ZΔE or Z-ICF
(exposure for 30 min)
75
ZΔE or Z-ICF
(exposure for 5 min)
WB: anti-RPTPβ

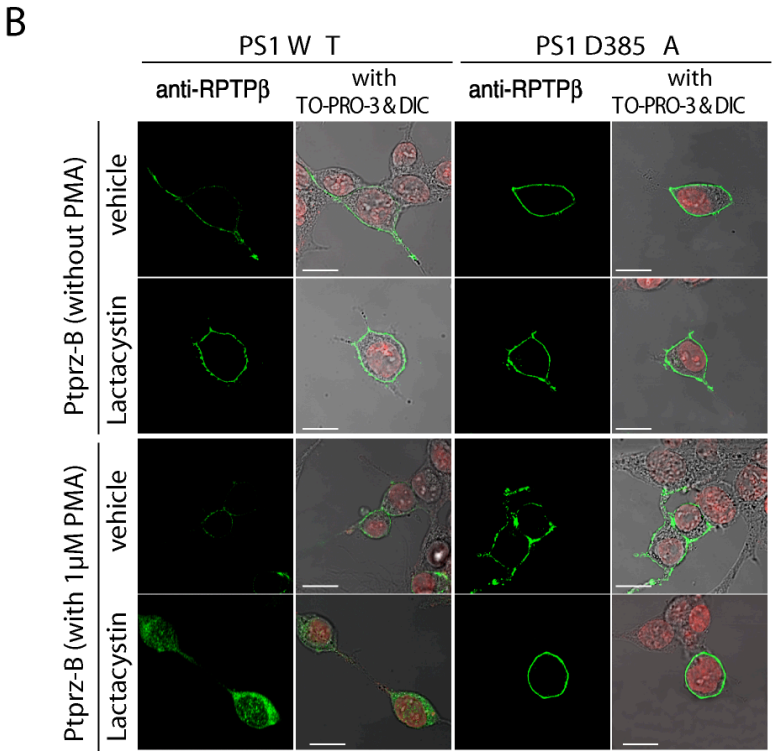
B
PS1 W T
PS1 D385 A
anti-RPTPβ
with TO-PRO-3 & DIC
anti-RPTPβ
with TO-PRO-3 & DIC
Ptprz-B (without PMA)
vehicle
Lactacystin
Ptprz-B (with 1μM PMA)
vehicle
Lactacystin

Fig. II-13. Summary of Ptprz fragments. A. Schematic representation of Ptprz isoforms. Molecular sizes of the chondroitin sulfate proteoglycan forms (CS-PG) and their core proteins after treatment with chondroitinase ABC (chABC) are shown. Regions corresponding to the epitopes of antibodies used in this study are indicated by vertical bars. We designated the proteolytic fragments as follows: Z_A-ECF or Z_B-ECF, the extracellular fragment of Ptprz-A or Ptprz-B; ZΔE, the membrane-tethered fragment of Ptprz-A and Ptprz-B; Z-ICF, the intracellular fragment cleaved from ZΔE. The cleavage sites are indicated by arrows (red, metalloproteinases including TACE and MMP-9; blue, presenilin/γ-secretase). Domains are highlighted in different colors: CAH, carbonic anhydrase-like domain; FNIII, fibronectin type III domain; PTP-D1 and PTP-D2, tyrosine phosphatase domains. B, Summary of the immunoreactive bands (*b* to *i*). Their designation, apparent molecular size, and specific antibodies for detection are shown.

A

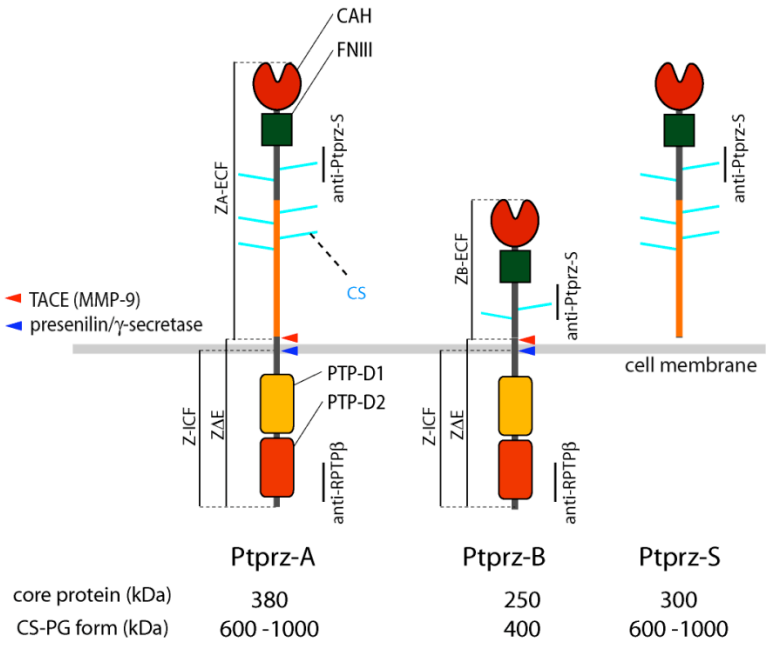

B

band	designation	apparent molecular size (kDa)	antibodies for detection
*a	Ptprz-A	380	anti-Ptprz-S, anti-RPTPβ
b	Ptprz-S or ZA-ECF	300	anti-Ptprz-S
c	Ptprz-B	250	anti-Ptprz-S, anti-RPTPβ
d	ZB-ECF	180	anti-Ptprz-S
e	Z-ECF100	100	anti-Ptprz-S
f	Z-ECF90	90	anti-Ptprz-S
g	Z-ECF70	70	anti-Ptprz-S
h/i	ZΔE or Z-ICF	77/73	anti-RPTPβ

Chapter III

Plasmin-mediated processing of protein tyrosine phosphatase receptor type Z is enhanced after kainate-induced seizures in the mouse brain

III.1 Introduction

Ptprz (also known as PTPζ or RPTPβ) is a receptor-type protein tyrosine phosphatase, which is predominantly expressed in the CNS. Ptprz is expressed in both neurons and glial cells (Shitani et al., 1998). *Ptprz*-deficient mice display impairments of hippocampal function in a maturation-dependent manner (Niisato et al.,2005; Tamura et al., 2006) and fragility of myelin in the CNS (Harroch et al., 2000), demonstrating its physiological importance.

Three isoforms of Ptprz are generated by alternative splicing from the *Ptprz* gene: The two transmembrane (receptor) isoforms, Ptprz-A and Ptprz-B, and the secretory isoform, Ptprz-S (also known as 6B4 proteoglycan or phosphacan) (Krueger et al., 1992; Levy et al., 1993; Maeda et al., 1994; Sakurai et al., 1996)), all of which are expressed as CSPGs in the brain (Nishiwiki et al., 1998). However, several features of the molecular profile of Ptprz have remained unclear. For instance, lower molecular weight species have been detected with a specific antibody against the extracellular region of Ptprz in the wild-type mouse brain (Shitani et al., 1998): As shown in Fig. III-1 (left panel), several bands (here, the bands are referred to as *b*-*g*) were clearly detected by anti-Ptprz-S in a brain extract prepared from wild-type adult mice (for the recognition site of the antibody, see Fig. III-4). Because these bands are not present in *Ptprz*-deficient mice (Shitani et al., 1998), they most likely represent the molecular species derived from the *Ptprz* gene. The bands of 300 kDa (band *b*) and 250 kDa (band *c*) represent the core proteins of Ptprz-S and Ptprz-B, respectively (Nishiwiki et al., 1998). In contrast, the core protein (380 kDa) of the full-length Ptprz-A was hardly detected in the adult brain extract (the position was indicated by arrowhead (*a*)

with asterisk in Fig. III-1) in spite of the significant expression at the transcription level (Maurel et al., 1994; Canoll et al., 1996), suggesting proteolytic processing of Ptprz-A.

In chapter II, I demonstrated metalloproteinase-mediated cleavage of the receptor isoforms of Ptprz *in vivo*, releasing the extracellular domain from the cell surface. It showed that the 180-kDa band (band *d* in Fig. III-1) represents the entire extracellular fragment of Ptprz-B (Z_B-ECF, see also Fig. III-4). From Ptprz-A, Z_A-ECF (300 kDa) is generated, which is indistinguishable from the secreted isoform, Ptprz-S, in size and antigenicity (see Fig. III-4). However, the other molecular species (bands *e*-*g*) still remained to be identified. In this chapter, I show that these low molecular species are generated via the proteolysis of Ptprz by plasmin, and that this process is evidently enhanced after kainate-induced seizures.

III.2 Materials and Methods

Pharmacological reagents

Plasmin was purchased from Sigma. GM6001 was from Calbiochem

Animal experiments

Adult wild-type and *Ptprz*-deficient mice (Shintani et al., 1998) backcrossed with the inbred C57BL/6 strain for more than ten generations were used. Kainic acid (35 mg per kg body weight, Sigma) was administered intraperitoneally, and behavioral changes including limbic motor seizures were observed for 1 h as described (Yuen et al., 2002). Tissues were isolated at 24 h after the administration. All animal experiments were performed according to the guidelines of Animal Care with approval by the Committee for Animal Research, National Institutes of Natural Sciences.

Cell Culture and DNA Transfection

HEK293T cells (human embryonic kidney epithelial cells) were grown and maintained in Dulbecco's modified Eagle's medium (DMEM) supplemented with 10% fetal bovine serum in a humidified incubator at 37˚C with 5% CO_2, and transfected with *Ptprz* expression plasmids by calcium-phosphate precipitation (Fujikawa et al., 2007). Full-length rat *Ptprz-A* (Maeda et al., 1994) was subcloned into the expression vector pZeoSV2 (Invitrogen) to yield pZeo-PTPζ-A. The expression plasmids for rat Ptprz-B (pZeoPTPζ) (Kawachi et al., 2001) and the N-terminal FLAG-tagged Ptprz-B (pZeo-FLAG-PTPζ) (Fujikawa et al., 2003) were described previously.

Mouse tissues and cultured cells were lysed with 1% NP-40 in 20 mM Tris-HCl, pH 8.0, 137 mM NaCl, 10 mM NaF, 1 mM sodium orthovanadate, and a EDTA-free protease inhibitor cocktail (complete EDTA-free, Roche), and then supernatants were collected by centrifugation at 15,000 *g* for 15 min. Digestion with chondroitinase ABC (chABC, Seikagaku Co.) was performed in 0.2 M Tris, 4 mM sodium-acetate, pH 7.5 for 1 h at 37°C; the enzyme was added at 60 μU per μg protein. The samples prepared as above were analyzed by Western blotting using anti-Ptprz-S rabbit serum (1:10,000) (Nishiwiki et al. 1998), mouse monoclonal anti-RPTPβ (250 ng/ml, BD Biosciences), or mouse monoclonal anti-FLAG M2 (Sigma) with an ECL Western blotting system (GE Healthcare). The epitope regions in Ptprz recognized by the antibodies are shown in Fig. III-4.

In vitro digestion analyses

In vitro digestion experiments with plasmin were performed using purified GST-Ptprz-B(151-827) protein, which is a glutathione S-transferase (GST) fusion protein comprising a partial extracellular region of Ptprz-B, the transmembrane segment, and a short intracellular segment; from Leu at 151 to Pro at 827 of rat Ptprz-B. The *E. coli* expression plasmid was prepared by subcloning the appropriate cDNA from pZeoPTPζ into pGEX-6P (GE Healthcare). The GST-Ptprz-B(151-827) protein was purified by glutathione affinity chromatography as decribed (Fujikawa et al., 2007).

III.3 Results

Proteolysis of phosphacan (Ptprz-S) was reported to occur in mice after seizures induced by kainic acid through the tissue plasminogen activator (tPA)/plasmin system, although characterization of the processing products was not performed (Wu et al., 2000). In this study, plasmin, but not tPA, was revealed to be responsible for the proteolysis of phosphacan by using tPA- and plasminogen-knockout mice. I examined the molecular nature of the receptor isoforms of Ptprz in the brain of wild-type mice administered kainic acid by Western blotting using anti-Ptprz-S. As shown in Fig. III-1 (left panel), in the cerebral cortex of mice which exhibited seizures (lanes *3* and *4*), there occurred a drastic increase in the band of 70 kDa (band *g*), along with the disappearance of other bands. In contrast, there was no such alteration in seizure-free (lanes *5* and *6*) or vehicle-treated (lanes *1* and *2*) mice. These results suggest that plasmin-mediated processing is mainly implicated in the production of the low molecular species (bands *e* and *g*) in the adult brain.

Plasmin-mediated cleavage of Ptprz-B

To directly test this view, HEK293T cells were transiently transfected with an expression construct of Ptprz-B and treated with plasmin. Here I first adopted Ptprz-B because it is predominantly detected in the adult brain at the protein level. As shown in Fig. III-2A, in the presence of plasmin, the full-length Ptprz-B in the cell membrane was processed with relatively high doses of plasmin and the lower bands appeared instead (top panel, lanes *2*-*7*; $Z_B\Delta170$, $Z_B\Delta150$, and $Z_B\Delta140$). In the culture medium, the immunoreactivity of Z_B-ECF (180 kDa) was detectable without any treatments

(bottom panel, lane *2*). Z_B-ECF was increased at the lowest dose (2.3 mU/ml; bottom panel, lane *3*), but rather decreased with higher doses of plasmin (bottom panel, lanes *3*-5). At relatively high doses of plasmin (38-150 mU/ml), Ptprz-B yielded a major band of 70 kDa (Z-ECF70) together with a band of 90 kDa (Z-ECF90) in the culture medium. Interestingly, the sizes of these two fragments corresponded to bands "*g*" and "*f*", respectively, in the brain tissue (see Fig. III-1). When the N-terminal FLAG-tagged Ptprz-B was expressed, both bands corresponding to Z-ECF90 and Z-ECF70 were detected besides Z_B-ECF (180 kDa) by anti-FLAG, as well as by anti-Ptprz-S, indicating that they are N-terminal extracellular fragments generated by the processing of the receptor isoform (Fig. III-2). On treatment with over 150 mU/ml of plasmin, two additional fragments of Z-ECF30 and Z-ECF27 were detected in the medium (Fig. III-3A, bottom panel). In contrast, there were no corresponding bands in the brain (see Fig. III-1).

In chapter II, I have already revealed that Z_B-ECF is produced by metalloproteinase-mediated cleavage of Ptprz-B, and that the basal production of Z_B-ECF itself is not affected by the treatment of cells with leupeptin which inhibits plasmin activit. Since plasmin has a potential to induce metalloproteinase activity (Monea et al., 2002), I performed the same experiment in the presence of GM6001, a broad-spectrum metalloproteinase inhibitor (Fig. III-3A, lanes *9-14*). Interestingly, cell treatment with GM6001 selectively inhibited the production of Z_B-ECF without affecting the generation of other fragments (Fig. III-3A, compare lanes *2-7* and lanes *9-14*). These results indicated that the metalloproteinase-mediated release of Z_B-ECF is induced by low doses of plasmin, but the released extracellular fragment is further processed at multiple sites at high doses of plasmin.

In vitro cleavage of Ptprz-B by plasmin

To further verify that plasmin directly cleaves the extracellular region of Ptprz-B thereby producing multiple fragments, we incubated a GST fusion protein (comprising a part of the extracellular region, the transmembrane segment, and a short portion of the intracellular region of Ptprz-B) with plasmin *in vitro*. As shown in Fig. III-4, plasmin cleaved the recombinant protein into four immunoreactive fragments of 80, 60, 20, and 17 kDa in a dose-dependent manner. Importantly, the pattern was very similar to that of Z-ECF90, Z-ECF70, Z-ECF30, and Z-ECF27 observed on the treatment of Ptprz-B with plasmin in the cell culture (see Fig. III-3A, bottom panel). We here analyzed the N-terminal sequence of the 60-kDa fragment by automated Edman sequencing (data not shown) and revealed that plasmin cleaves between Lys (478) and Thr (479) residues located downstream of the fibronectin type III domain (see Fig. III-5).

Plasmin-mediated cleavage of Ptprz-A

Although the full-length Ptprz-A of 380 kDa has been scarcely observed at the protein level in the adult brain (see Fig. III-1 and (Nishiwaki et aal., 1998)), there exists substantial expression of the transcript (Maurel et al., 1994; Canoll, et al., 1996). This strongly suggests the massive proteolytic processing of this receptor isoform under physiological conditions. In line with this view, the disappearance of full-length Ptprz-A expressed in HEK293T cells was observed at a 30-60 fold lower concentration of plasmin (Fig. III-3B, top panel), as compared with that of Ptprz-B (Fig.III-3A, top panel). As in Ptprz-B, Z_A-ECF of 300 kDa, which corresponds to the entire extracellular fragment (see Fig. III-5) was increased by plasmin treatment at relatively

low doses (Fig. III-2B, bottom panel). However, the production of Z_A-ECF was followed by the formation of several immunoreactive fragments (Z-ECF280 to Z-ECF150), suggesting additional cleavage sites in Ptprz-A. These sites should be located within the region deleted in Ptprz-B: The presence of multiple primary cleavage sites may explain the higher sensitivity of the full-length Ptprz-A and Z_A-ECF to plasmin. As with Ptprz-B, the generation of Z_A-ECF from Ptprz-A was selectively inhibited by GM6001 (Fig. III-3B, bottom panel, lanes *9-14*).

Mapping of plasmin cleavage sites in the extracellular region of Ptprz

Both the cell-based assays (Fig. III-3) and the *in vitro* digestion experiments of recombinant proteins (Fig. III-4) thus indicated that plasmin cleaves the extracellular regions of the receptor isoforms of Ptprz at multiple sites. To determine the location of cleavage sites by plasmin, we reprobed the blots of the cell extracts with anti-RPTPβ which recognizes the intracellular region (as for the epitope region, see Fig. III-5). As shown in the middle panels of Fig. III-3, the bands detected by anti-RPTPβ should represent the membrane-tethered C-terminal fragment (Z_BΔEs, Z_AΔEs, or ZΔE) produced from Ptprz-B, Ptprz-A, or both receptors, respectively (see also Fig. 4): ZΔE was found to be the common counterpart fragment of Z_B-ECF and Z_A-ECF produced by metalloproteinase-mediated cleavage (see chapter II). Based on the size and antigenicity of the fragments detected, we estimated cleavage sites by plasmin as shown in Fig. III-5. The secreted isoform, Ptprz-S, has the same structure as the entire extracellular region of Ptprz-A (Z_A-ECF) except for the C-terminus, and therefore, these two proteins should be expected to have the same processing pattern.

III.4 Discussion

Recent reports have uncovered new functions for the tPA/plasmin system in the physiology and pathology of the CNS (Melchor and Strickland, 2005): tPA expression is up-regulated in the rat hippocampus after seizure, kindling, and long-term potentiation (LTP) (Qian et al., 1993). Plasminogen is converted to its active form, plasmin, through proteolytic cleavage by tPA. tPA is produced by neurons and microglia, whereas plasminogen is expressed by neurons (Tsirka et al., 1997). The tPA/plasmin system is implicated in neuronal cell death after exitotoxic injury: Generation of plasmin by tPA leads to the degradation of extracellular matrix (ECM) and cell surface components, and induces neuronal degeneration (see Tsirka, 2002 for a review). The secreted Ptprz isoform, phosphacan (Ptprz-S), is one of the major CSPGs in the brain (Maurel et al., 1994; Maeda et al., 1995) and also a major component of the ECM. Phosphacan (Ptprz-S) is a repulsive substratum and promotes neurite outgrowth in rat primary cultured cortical neurons (Maeda et al., 1996). The enhancement of the proteolytic processing of Ptprz in mice which exhibited seizures suggests its pathological role in the kainate-induced damage.

However, I should emphasize here that the proteolytic fragments are evidently present in the normal brain, and therefore, the processing of Ptprz occurs under physiological conditions (Fig. III-1). Interestingly, tPA is released from the dendritic spines of hippocampal neurons in an activity-dependent manner (Lochner et al., 2006). Mice lacking tPA exhibit a deficit in late-phase of LTP (L-LTP) and impairment in hippocampal learning ability (Frey et al., 1996; Huang et al., 1996). Mice lacking plasminogen also exhibited severe impairments in L-LTP (Pang et al., 2004). One

conspicuous defect in adult *Ptprz*-deficient mice is an enhancement of LTP in the CA1 region of the hippocampus without affecting basal synaptic transmission (Niisato et al., 2005, together with learning deficits ((Kawachi et al., 1999;Fukada et al., 2005), . Ptprz receptor isoforms interact with the PSD95 family including PSD95, SAP97, and SAP102 through the carboxyl-terminal PDZ-binding motif (Kawachi et al., 1998; Fukada et al., 2005), and are assumed to be located in the postsynaptic density of central synapses. These findings suggest that the activity-dependent proteolytic processing of the extracellular regions Ptprz by the tPA/plasmin system facilitates synaptic remodeling, and thereby plays a role in learning and memory.

In addition, the extracellular processing of Ptprz might produce a ligand for the reverse signaling at the synapse. The extracellular CAH-like domain of Ptprz reportedly binds to contactin (Pele et al., 1995). The distribution of Ptprz is altered in the hippocampus of *contactin*-deficient mice, which exhibit significant impairments in paired-pulse facilitation (PPF), a form of short-term synaptic plasticity, and long-term depression (LTD) (Murai et al., 2002). Furthermore, interaction of the extracellular region of Ptprz with other cell adhesion molecules such as N-CAM and L1/Ng-CAM (see (Pele et al., 1998) for a review) may also play roles in the synaptic targeting and synaptic regulation. It is thus possible that proteolytic processing of Ptprz contributes to hippocampus-dependent memory by modulating long-lasting synaptic plasticity, but confirmation of this awaits further study.

Fig. III-1. Increase in the 70-kDa fragment of Ptprz in the adult mouse brain after kainate-induced seizures. Cerebral cortex extracts (5 μg protein) prepared from wild-type mice after the administration of kainic acid (or vehicle) were treated with chABC before SDS-PAGE, and then analyzed by Western blotting usig anti-Ptprz-S (left panel). The resolved proteins were visualized by staining the gel with coomassie brilliant blue R-250 (right panel). In the experimental conditions, the systemic injection of kainic acid (KA) induced seizures in most of the mice within 1 h (18/20), and 15 of these mice died by 24 h post-injection. Mice with seizures (lanes *3* and *4*), mice without seizures (lanes *5* and *6*), and vehicle-treated mice (con, lanes *1* and *2*) are shown. The detected bands are indicated by arrowheads and a square bracket. Several unidentified immunoreactive bands between 140 and 100 kDa are indicated by square bracket (*e*). While the core protein of Ptprz-A is not detected in the tissue extract, the corresponding position is indicated by arrowhead (*a*) with asterisk.

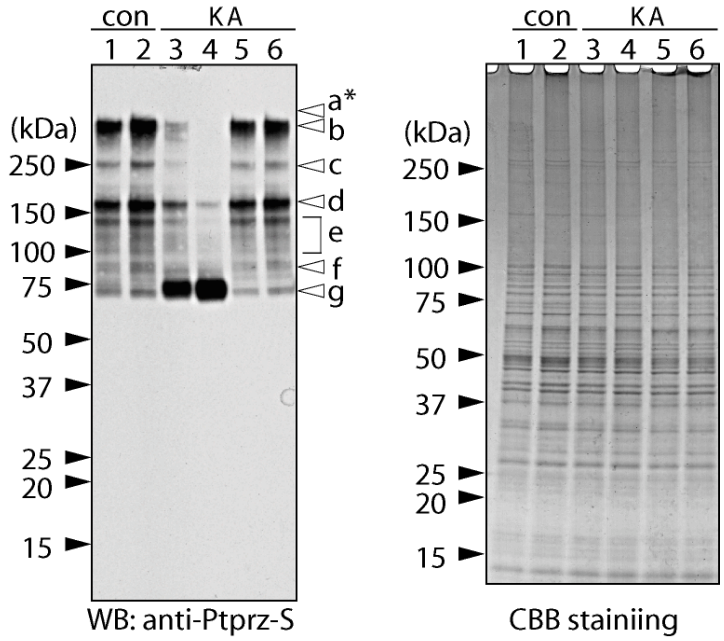
con
KA
1 2 3 4 5 6
(kDa)
250
150
100
75
50
37
25
20
15
a*
b
c
d
e
f
g
WB: anti-Ptprz-S
CBB stainiing

Fig. III-2. Plasmin-mediated cleavage of the extracellular region of Ptprz. HEK293T cells were transiently transfected with the expression construct for the N-terminal FLAG-tagged Ptprz-B (lanes *2-7* and *9-14*) or the control empty vector (pZeoSV2) (Moc, lanes *1* and *8*). As in Fig. III-3, 24 h after transfection, cells were preincubated with fresh serum-free medium for 40 min, incubated further in the presence or absence of GM6001 for 20 min, and then treated with the indicated amounts of plasmin for 1 h. Cultured media were analyzed by Western blotting with anti-FLAG M2 (Sigma), and followed by reprobing with anti-Ptprz-S. The bands generated by proteolytic processing are indicated by arrowheads with their names as shown in Fig. III-5. Anti-FLAG detected a band at 60 kDa (arrow with asterisk), which was not recoginized by anti-Ptprz-S, suggesting the presence of additional proteolytic cleavage sites in the extracelular region of Ptprz.

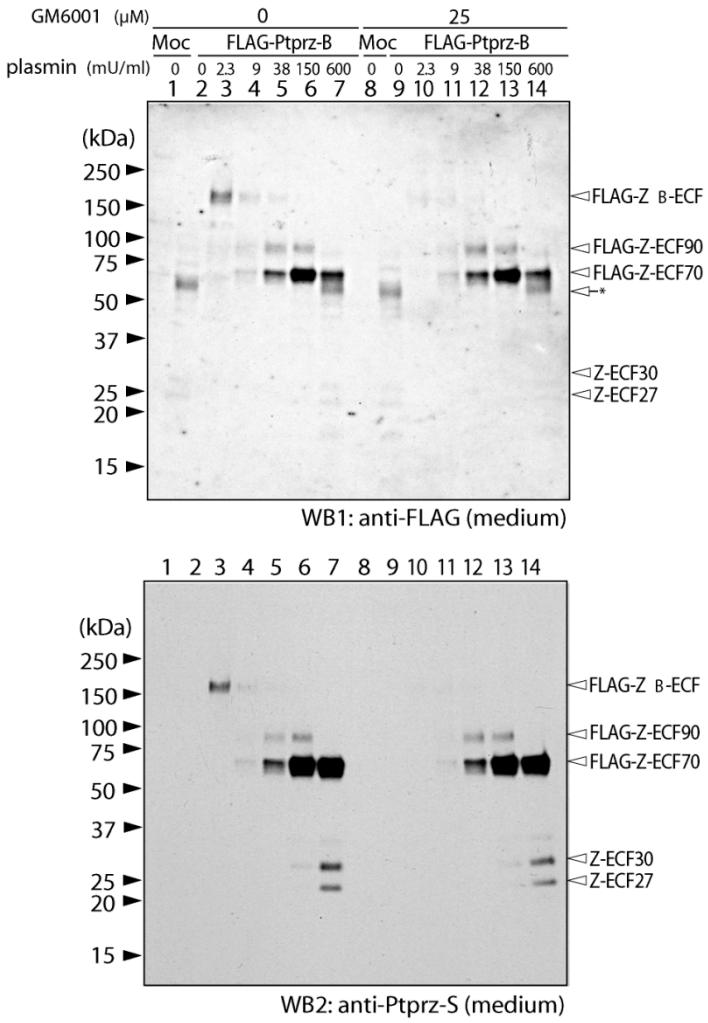
GM6001 (μM)
0
25
Moc
FLAG-Ptprz-B
Moc
FLAG-Ptprz-B
plasmin (mU/ml)
0 0 2.3 9 38 150 600 0 0 2.3 9 38 150 600
1 2 3 4 5 6 7 8 9 10 11 12 13 14
(kDa)
250
150
100
75
50
37
25
20
15
FLAG-Z B-ECF
FLAG-Z-ECF90
FLAG-Z-ECF70
*
Z-ECF30
Z-ECF27
WB1: anti-FLAG (medium)
1 2 3 4 5 6 7 8 9 10 11 12 13 14
(kDa)
250
150
100
75
50
37
25
20
15
FLAG-Z B-ECF
FLAG-Z-ECF90
FLAG-Z-ECF70
Z-ECF30
Z-ECF27
WB2: anti-Ptprz-S (medium)

Fig. III-3. Plasmin-mediated cleavage of the extracellular region of Ptprz. A, HEK293T cells were transiently transfected with the expression construct for Ptprz-B (lanes *2-7* and *9-14*) or the control empty vector pZeoSV2 (Moc, lanes *1* and *8*). Twenty-four hours after transfection, cells were preincubated with fresh serum-free medium for 40 min, incubated further for 20 min in the presence or absence of GM6001, and then treated with the indicated amounts of plasmin for 1 h. B, HEK293T cells transfected with the expression construct for Ptprz-A (or the control vector) were analyzed as in (A). Unlike Ptprz-B, when Ptprz-A was expressed in HEK293T cells, the mature receptor protein was highly modified with CS (data not shown). Therefore, the samples were treated with chABC just before SDS-PAGE. Cell extract was analyzed by Western blotting with anti-Ptprz-S (top panels) followed by reprobing with anti-RPTPβ (middle panels). Cultured media were analyzed with anti-Ptprz-S (bottom panels). The bands generated by proteolytic processing from mature Ptprz isoforms are indicated by arrowheads with their names as shown in Fig. III-4. The protein bands indicated by arrows with asterisks are immature or abnormally processed products in the cell: They are usually observed as described in (Nishiwaki et al., 1998) when the receptor isoforms are exogenously expressed. These products are apparently localized in the cytoplasm, because they are resistant to the trypsin treatment of cells (data not shown). In addition, their signal intensities were not altered by the plasmin treatment. Non-specific bands are indicated by filled arrowheads.

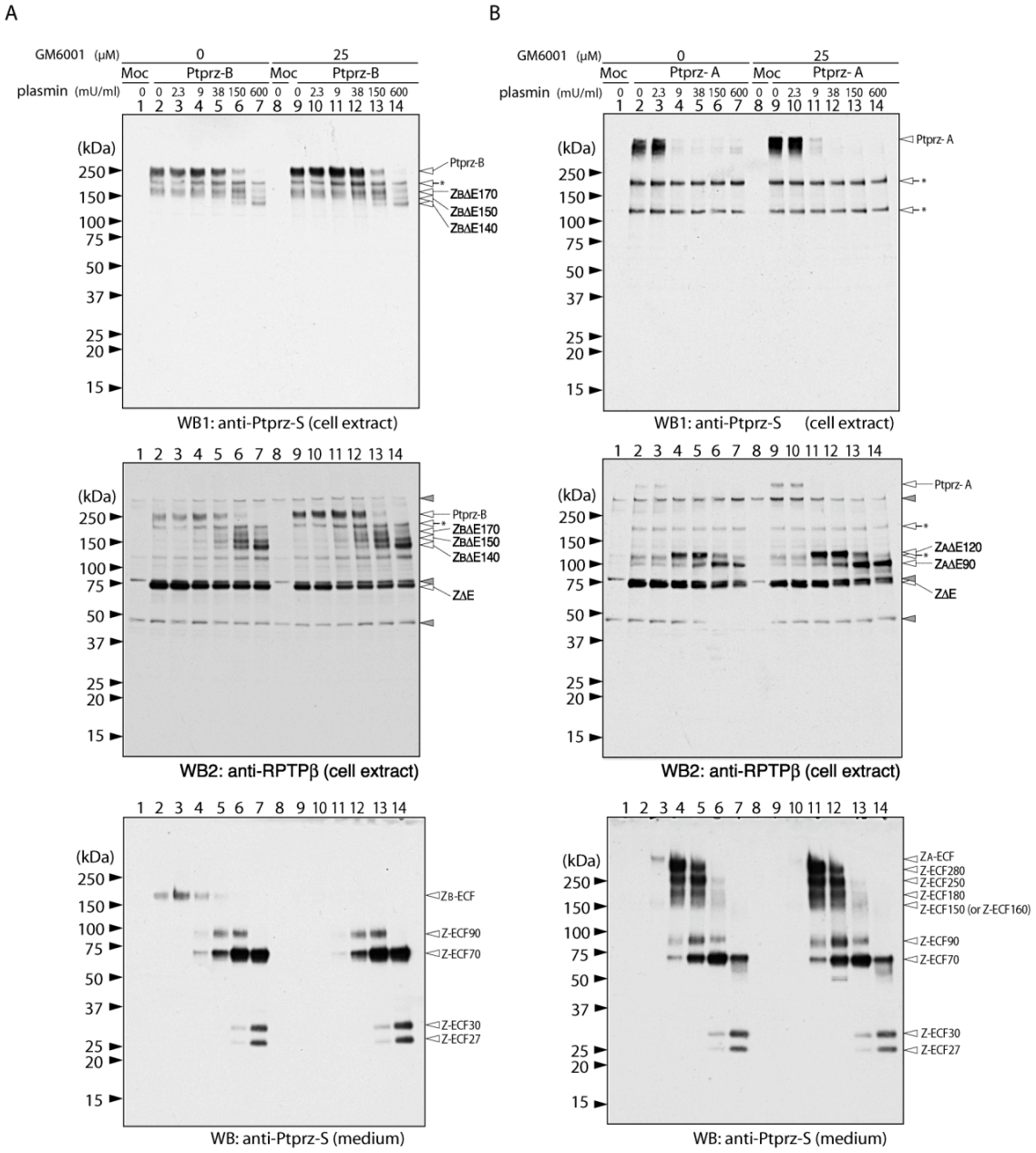
A
B
GM6001 (μM)
0
25
Moc
Ptprz-B
Ptprz- A
plasmin (mU/ml)
0 0 2.3 9 38 150 600
1 2 3 4 5 6 7 8 9 10 11 12 13 14
(kDa)
250
150
100
75
50
37
25
20
15
Ptprz-B
ZBΔE170
ZBΔE150
ZBΔE140
Ptprz- A
ZAΔE120
ZAΔE90
ZΔE
WB1: anti-Ptprz-S (cell extract)
WB2: anti-RPTPβ (cell extract)
ZB-ECF
Z-ECF90
Z-ECF70
Z-ECF30
Z-ECF27
ZA-ECF
Z-ECF280
Z-ECF250
Z-ECF180
Z-ECF150 (or Z-ECF160)
WB: anti-Ptprz-S (medium)

Fig. III-4. *In vitro* digestion of the extracellular region of Ptprz with plasmin. GST-Ptprz-B(151-827) (0.5 μg) was incubated with the indicated amounts of plasmin and time at 30°C in a final volume of 15 μl of 50 mM HEPES, pH 8.0. The samples were then analyzed by Western blotting with anti-Ptprz-S. Arrowheads (gray) indicate non-specific immunoreactive proteins that were copurified with the intact protein. A schematic view of Ptprz-B is shown with the region of the recombinant protein (vertical line).

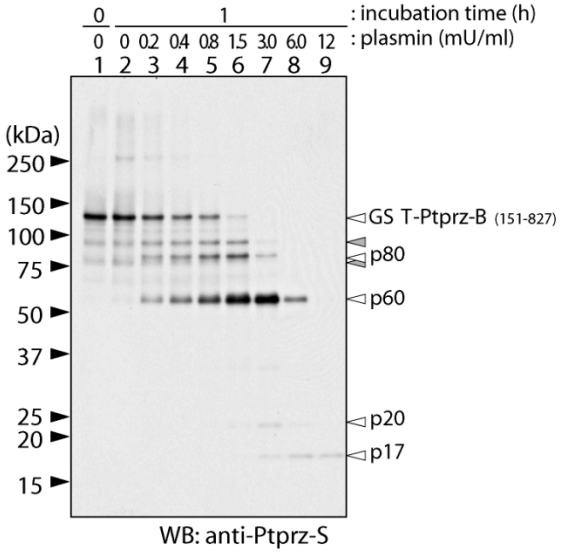
0
1
: incubation time (h)
0 0 0.2 0.4 0.8 1.5 3.0 6.0 12
: plasmin (mU/ml)
1 2 3 4 5 6 7 8 9
(kDa)
250
150
100
75
50
37
25
20
15
GS T-Ptprz-B (151-827)
p80
p60
p20
p17
WB: anti-Ptprz-S

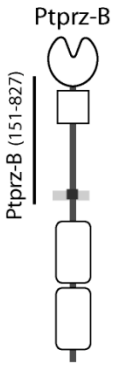
Ptprz-B
Ptprz-B (151-827)

Fig. III-5. Predicted sites of cleavage by plasmin in the extracellular region of Ptprz. Schematic representation of Ptprz isoforms with mapped plasmin cleavage sites from the results in Fig. II-2 and Fig. III-4. Z_A-ECF, Z_B-ECF (the extracellular fragment of Ptprz-A and Ptprz-B, respectively), and ZΔE (the membrane-tethered fragment of Ptprz-A/-B) are also shown in blue at the left. These fragments are generated by metalloproteinase-mediated cleavage (see chapter II). Domains of the core proteins are highlighted in different colors: CAH (red), carbonic anhydrase-like domain; FNIII (blue), fibronectin type III domain; PTP-D1 (orange) and PTP-D2 (green), protein tyrosine phosphatase domain. Regions corresponding to the epitopes of antibodies used in this study are indicated by vertical lines.

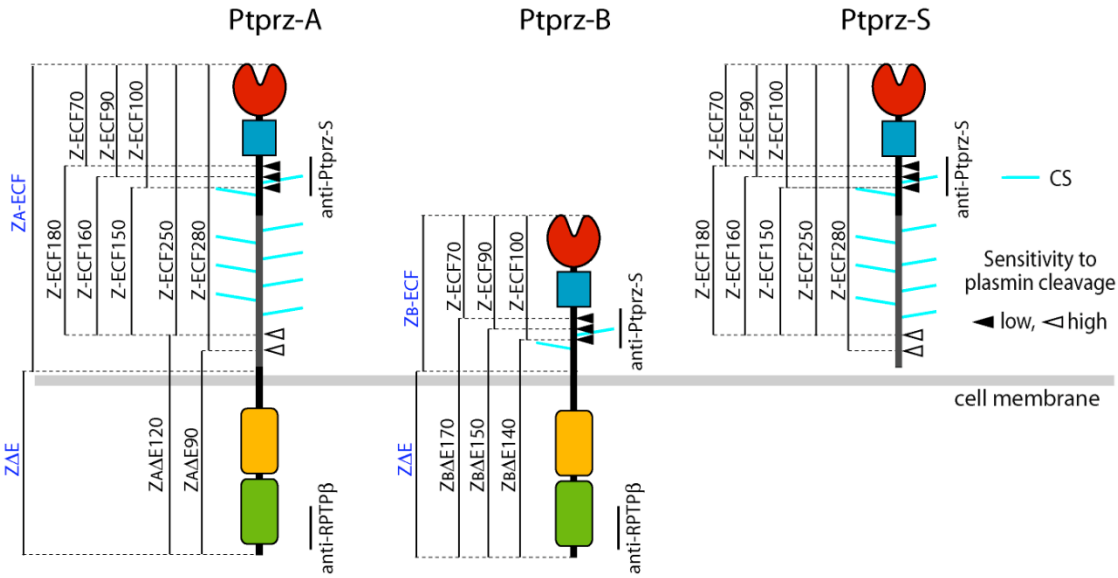
Ptprz-A
Ptprz-B
Ptprz-S
ZA-ECF
Z-ECF70
Z-ECF90
Z-ECF100
Z-ECF180
Z-ECF160
Z-ECF150
Z-ECF250
Z-ECF280
anti-Ptprz-S
ZAΔE120
ZAΔE90
ZΔE
anti-RPTPβ
ZB-ECF
ZBΔE170
ZBΔE150
ZBΔE140
CS
Sensitivity to
plasmin cleavage
◀ low, ◁ high
cell membrane

Chapter IV

Conclusion and perspectives

IV.1 Conclusion and Perspectives

An interesting feature of the receptor isoforms of Ptprz is the presence of extra splice isoforms that has a deletion of 7 amino-acid stretch encoded by exon 16, which is adjacent to the helix-turn-helix segment (termed "wedge region") in the intracellular juxtamembrane region (Li et al., 1998). When PSD fraction was purified from the cerebral cortex, I found that the C-terminal proteolytic fragment (Z-ICR) of the exon-16 deleted forms, but not that of the non-deleted form, is selectively enriched in the PSD fraction (Fig. IV-1A). PSD95 was pulled down more efficiently with exon 16-deleted ($Z\text{-}ICR_{\Delta ex16}$) than with the non-deleted (Z-ICR) recombinant proteins from the P2 fraction of mouse brains (Fig. IV-1B).

In the present study, I provide evidence that Ptprz receives regulated proteolytic in the adult mouse CNS, leading us to a model as in Fig. IV-1C. At the central synapse, ectodomain cleavage of Ptprz receptor-isoforms by metalloproteinase including TACE generates a membrane-associated fragment, and then releases the cytoplasmic domain by γ-secretase from the plasma membrane. The cytoplasmic domain is found in the cytoplasm and also in the nucleus, suggesting a novel signaling pathway of Ptprz. In addition, the extracellular fragments ($Z_{A/B}$-ECF) may function as ligand molecules that may function as a reverse signaling to the presynaptic receptors such as contactin, though they are further digested by metalloproteinases including plasmin.

A novel aspect of the function of Ptprz is proposed in the present study. The cytoplasmic domain is found to translocate to the nucleus after ectodomain shedding and RIP. This change of cellular compartmentation may recruit and regulate a unique set of molecules that locate only in the nucleus. It is important to understand whether

Ptprz plays direct role for gene transcription and what kinds of gene are regulated?

Another question is how cytoplasmin domain of Ptprz translocates to the nucleus? The cyoplasmic domain of Ptprz contains no known nuclear localization sequence (NLS). It seems that a docking protein (whether it contains NLS or forms a tripartite complex with another protein with NLS) is necessary to mediate its nuclear translocation. Most of the transmembrane proteins located in the synapse interact with PDZ-containing proteins to form a large complex. Some of them are reportedly shed and their cytoplasmic domains are detected in the nucleus. However, the exact mechanism is not known. Is there a common mechanism for the synaptic transmembrane protein to be released from the large complex and regulate gene expression directly?

Our group very recently identified ErbB4 as a substrate for Ptprz (Fujikawa et al., 2007). It has been reported that ErbB4 undergoes ectodomain cleavage by TACE (Cheng et al., 2003): Of note is that both ErbB4 and TACE harbor a PDZ-binding motif at the C-terminus, and thereby associate with members of the PSD95 family (Huang et al., 2000; Peiretti et al., 2003) together with Ptprz. Upon neuregulin-induced activation of ErbB4, presenilin-dependent cleavage of ErbB4 occurs. Subsequently, its intracellular domain (E4ICD) forms a signaling complex (Ni et al., 2001) and reportedly translocates into the nucleus to repress the expression of some glial genes, including a protein marker of astrocyte GFAP, by binding to the promoters *in vivo* (Sardi et al., 2006). I have found that there is a decrease in GFAP expression in the developmental stage of *Ptprz*-deficient mice. It raises the possibility that Ptprz may play role in the function of E4ICD in the nucleus. More studies are need to understand the novel functions of Ptprz.

Fig. IV-1. Selective localization of the exon 16-deleted forms in the postsynaptic density (PSD) in the brain. A, Adult mouse cortex homogenates (total) were subjected to sequential centrifugations to yield synaptosomes (P2) and PSD fraction, and analyzed by Western blotting. B, Pull-down experiments of PSD95 using GST fusion proteins of the whole intracellular regions of the non-deleted form (Z-ICR) and exon 16-deleted form (Z-ICR$_{\Delta ex16}$) from the cerebral synaptosomal fraction. The pull-down samples were analyzed by Western blotting. C, Schematic images of the proteolytic processing of the two receptor variants of Ptprz with and without exon 16 at the central synapses. Metalloproteinase-mediated ectodomain shedding of Ptprz-A/B releases the extracellular domain $Z_{A/B}$-ECF from the cell surface, and produces the membrane-tethered counterpart ZΔE. $Z_{A/B}$-ECF (or their fragments) may function as ligands for the presynaptic receptor like contactin for reverse signaling **(1)**, or may inhibit integrin signaling **(2)**. Almost all Ptprz-A is cleaved in the adult brain, and therefore, Ptprz-B seems to be mainly processed in association with synaptic activity. Although plasmin may enhance the ectodomain shedding of Ptprz through activation of metalloproteinases, the main role of plasmin appears to degrade Ptprz, together with various extracellular matrix proteins, into further small fragments. Of note is that the exon 16-deleted forms, but not non-deleted forms, are exclusively localized to the PSD due to the higher affinity with PSD95. Thus, the ectodomain shedding of Ptprz-A/B presumably leads to enhancement of the PTPase activity and dephosphorylation of the substrate molecules such as p190 RhoGAP in PSD **(3)**. Finally, ZΔEs are subsequently digested by γ-secretase and the cytoplasmic fragment is released from the plasma membrane to not only the cytoplasm but the nucleus, suggesting a novel signaling pathway of Ptprz **(4)** leading to long-lasting synaptic changes.

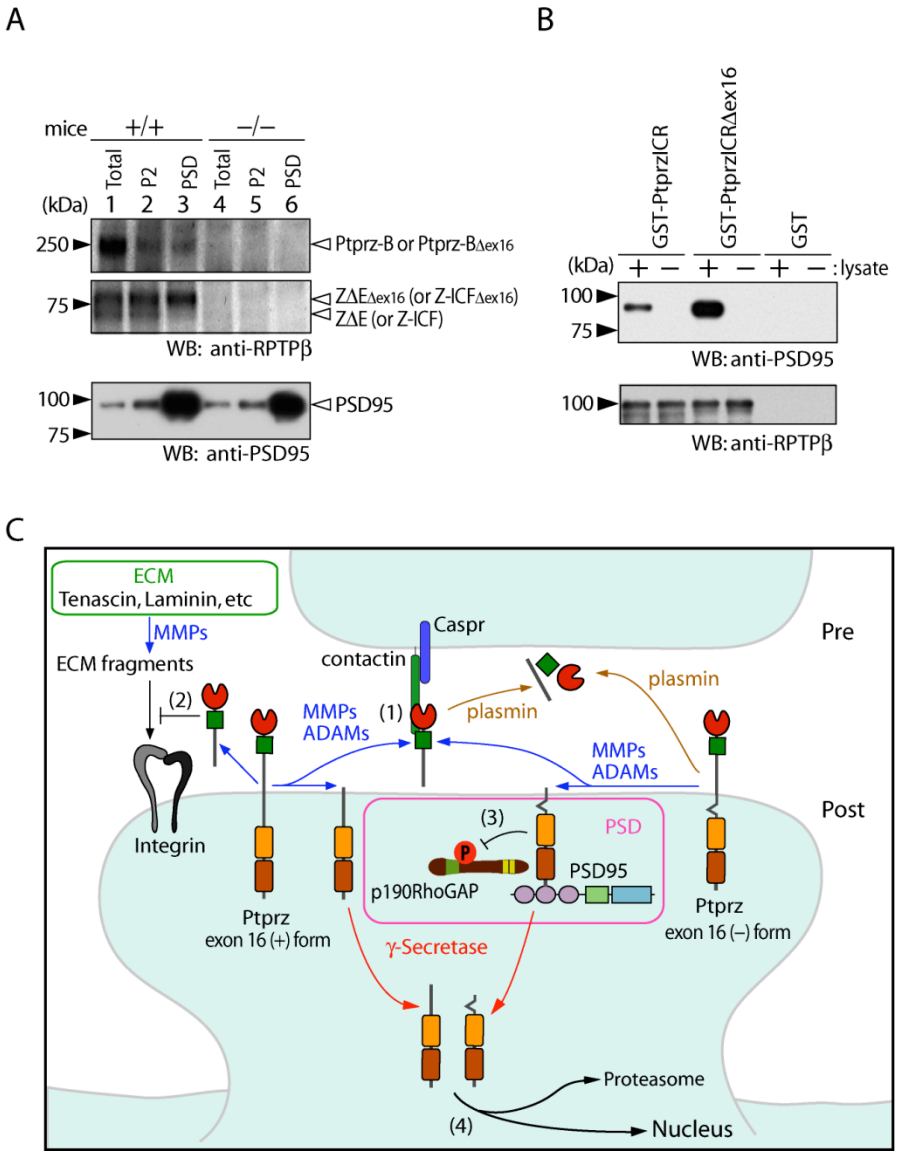
A
mice
+/+
−/−
Total
P2
PSD
Total
P2
PSD
(kDa)
1
2
3
4
5
6
250
Ptprz-B or Ptprz-BΔex16
75
ZΔEΔex16 (or Z-ICFΔex16)
ZΔE (or Z-ICF)
WB: anti-RPTPβ
100
75
PSD95
WB: anti-PSD95
B
GST-PtprzICR
GST-PtprzICRΔex16
GST
(kDa)
+
−
+
−
+
−
: lysate
100
75
WB: anti-PSD95
100
WB: anti-RPTPβ
C
ECM
Tenascin, Laminin, etc
MMPs
ECM fragments
(2)
Integrin
Caspr
contactin
MMPs
ADAMs
(1)
plasmin
plasmin
MMPs
ADAMs
Pre
Post
(3)
PSD
P
p190RhoGAP
PSD95
Ptprz
exon 16 (+) form
γ-Secretase
Ptprz
exon 16 (−) form
Proteasome
(4)
Nucleus

Acknowledgements

My sincere gratitude is reserved to my principle supervisor, Prof. M. Noda for his kind guidance and encouraging me along the way. I would also like to thank Dr. A. Fujikawa for patiently making suggestions and Dr. H. Shimizu and Dr. R. Suzuki for their technical help. I am grateful to have support from Miss R. Kodama.

Special thank to Dr. J. Arribas for CHO, CHO-M2 and CHO-M2/TACE cell lines and Dr. T Ikeuchi T for the HEK/PS1-WT and HEK/PS1DA cell lines.

I am much indebted to my parents and dedicated my work to them.

References

Alonso A, Sasin J, Bottini N, Friedberg I, Friedberg I, Osterman A, Godzik A, Hunter T, Dixon J, Mustelin T. (2004) Protein tyrosine phosphatases in the human genome. Cell 117:699-711.

Anders L, Mertins P, Lammich S, Murgia M, Hartmann D, Saftig P, Haass C, Ullrich A (2006) Furin-, ADAM 10-, and γ-secretase-mediated cleavage of a receptor tyrosine phosphatase and regulation of γ-catenin's transcriptional activity. Mol Cell Biol 26:3917-3934.

Arribas J, Borroto A (2002) Protein ectodomain shedding. Chem Rev 102:4627-4637.

Bats C, Groc L, Choquet D (2007) The interaction between Stargazin and PSD-95 regulates AMPA receptor surface trafficking. Neuron 53:719–734.

Bernard-Pierrot I, Héroult M, Lemaître G, Barritault D, Courty J, Milhiet PE (1999) Glycosaminoglycans promote HARP/PTN dimerization. Biochem Biophys Res Commun 266:437-442.

Bilwes AM, den Hertog J, Hunter T, Noel JP (1996) Structural basis for inhibition of receptor protein tyrosine phosphatase-α by dimerization. Nature 382:555–559.

Black RA, Rauch CT, Kozlosky CJ, Peschon JJ, Slack JL, Wolfson MF, Castner BJ, Stocking KL, Reddy P, Srinivasan S, Nelson N, Boiani N, Schooley KA, Gerhart M, Davis R, Fitzner JN, Johnson RS, Paxton RJ, March CJ, Cerretti DP (1997) A metalloproteinase disintegrin that releases tumour-necrosis factor-alpha from cells. Nature 385:729-33.

Blobel CP (2005) ADAMs: key components in EGFR signalling and development. Nat Rev Mol Cell Biol 6:32-43.

Borroto A, Ruíz-Paz S, de la Torre TV, Borrell-Pagès M, Merlos-Suárez A, Pandiella A,

Blobel CP, Baselga J, Arribas J (2003) Impaired trafficking and activation of tumor necrosis factor-α-converting enzyme in cell mutants defective in protein ectodomain shedding. J Biol Chem 278:25933-25939.

Brachmann R, Lindquist PB, Nagashima M, Kohr W, Lipari T, Napier M, Derynck R (1989) Transmembrane TGF-alpha precursors activate EGF/TGF-alpha receptors. Cell 56:691-700.

Brinckerhoff CE, Matrisian LM (2002) Matrix metalloproteinases: a tail of a frog that became a prince. Nat Rev Mol Cell Biol 31:207–214.

Canoll PD, Petanceska S, Schlessinger J, Musacchio JM (1996) Three forms of RPTP-β are differentially expressed during gliogenesis in the developing rat brain and during glial cell differentiation in culture. J Neurosci Res 44:199-215.

Cornell RA, Eisen JS (2005) Notch in the pathway: the roles of Notch signaling in neural crest development. Semin Cell Dev Biol 16:663–672.

Chang JH, Gill S, Settleman J, Parsons SJ (1995) c-Src regulates the simultaneous rearrangement of actin cytoskeleton, p190RhoGAP, and p120RasGAP following epidermal growth factor stimulation. J Cell Biol 130:355–368.

Cheng QC, Tikhomirov O, Zhou W, Carpenter G (2003) Ectodomain cleavage of ErbB-4: characterization of the cleavage site and m80 fragment. J Biol Chem 278:38421-38427.

Cross AK, Woodroofe MN (1999) Chemokine modulation of matrix metalloproteinase and TIMP production in adult rat brain microglia and a human microglial cell line in vitro. Glia 28:183–189.

Czernilofsky AP, Levinson AD, Varmus HE, Bishop JM, Tischler E, Goodman HM (1980) Nucleotide sequence of an avian sarcoma virus oncogene (src) and

proposed amino acid sequence for gene product. Nature 287:198–203.

Dityatev A, Schachner M (2006) The extracellular matrix and synapses. Cell Tissue Res 326:647-654.

Dobrosotskaya I, Guy RK, James GL (1997) MAGI-1, a membrane-associated guanylate kinase with a unique arrangement of protein-protein interaction domains. J Biol Chem 272:31589–31597.

Ethell IM, Ethell DW (2007) Matrix metalloproteinases in brain development and remodeling: synaptic functions and targets. J Neurosci Res 85:2813-2823.

Ferguson TA, Muir D (2000) MMP-2 and MMP-9 increase the neuritepromoting potential of Schwann cell basal laminae and are upregulated in degenerated nerve. Mol Cell Neurosci 16:157–167.

Flannery CR (2006) MMPs and ADAMTSs: functional studies. Front Biosci 11:544–569.

Frolichsthal-Schoeller P, Vescovi AL, Krekoski CA, Murphy G, Edwards DR, Forsyth P (1999) Expression and modulation of matrix metalloproteinase-2 and tissue inhibitors of metalloproteinases in human embryonic CNS stem cells. NeuroReport 10:345–351.

Fujikawa A, Shirasaka D, Yamamoto S, Ota H, Yahiro K, Fukada M, Shintani T, Wada A, Aoyama N, Hirayama T, Fukamachi H, Noda M (2003) Mice deficient in protein tyrosine phosphatase receptor type Z are resistant to gastric ulcer induction by VacA of *Helicobacter pylori*. Nat Genet 33:375-381.

Fujikawa A, Chow JPH, Shimizu H, Fukada M, Suzuki R, Noda M (2007) Tyrosine phosphorylation of ErbB4 is enhanced by PSD95 and repressed by protein tyrosine phosphatase receptor type Z. J Biochem 142:343-350.

Fukada M, Kawachi H, Fujikawa A, Noda M (2005) Yeast substrate-trapping system for isolating substrates of protein tyrosine phosphatases: Isolation of substrates for protein tyrosine phosphatase receptor type z. Methods 35:54-63.

Fukada M, Fujikawa A, Chow JPH, Ikematsu S, Sakuma S, Noda M (2006) Protein tyrosine phosphatase receptor type Z is inactivated by ligand-induced oligomerization. FEBS Lett 580:4051-4056.

Fukazawa Y, Saitoh Y, Ozawa F, Ohta Y, Mizuno K, Inokuchi K (2003) Hippocampal LTP is accompanied by enhanced F-actin content within the dendritic spine that is essential for late LTP maintenance in vivo. Neuron 38:447-460.

Garwood J, Heck N, Reichardt F, Faissner A (2003) Phosphacan short isoform, a novel non-proteoglycan variant of phosphacan/receptor protein tyrosine phosphatase-ζ, interacts with neuronal receptors and promotes neurite outgrowth. J Biol Chem 278:24164-24173.

Goddard DR, Bunning RA,Woodroofe MN (2001) Astrocyte and endothelial cell expression of ADAM 17 (TACE) in adult human CNS. Glia 34:267–271.

Gottschall PE Deb S (1996) Regulation of matrix metalloproteinase expression in astrocytes, microglia and neurons. Neuroimmunomodulation 3:69–75.

Guan KL, Haun RS, Watson SJ, Geahlen RL, Dixon JE (1990) Cloning and expression of a protein-tyrosine-phosphatase. Proc Natl Acad Sci USA 87:1501–1505

Hall A (1998) Rho GTPases and the actin cytoskeleton. Science 279:509-514.

Harroch S, Palmeri M, Rosenbluth J, Custer A, Okigaki M, Shrager P, Blum M, Buxbaum JD, Schlessinger J (2000) No obvious abnormality in mice deficient in receptor protein tyrosine phosphatase β. Mol Cell Biol 20:7706-7715.

Hartmann D, de Strooper B, Serneels L, Craessaerts K, Herreman A, Annaert W,

Umans L, Lubke T, Lena Illert A, von Figura K, Saftig P, (2002) The disintegrin/metalloprotease ADAM 10 is essential for Notch signalling but not for alpha-secretase activity in fibroblasts. Hum Mol Genet 11:2615–2624.

Huang YZ, Won S, Ali DW, Wang Q, Tanowitz M, Du QS, Pelkey KA, Yang DJ, Xiong WC, Salter MW, Mei L (2000) Regulation of neuregulin signaling by PSD-95 interacting with ErbB4 at CNS synapses. Neuron 26:443-455.

Jin G, Huang X, Black R, Wolfson M, Rauch C, McGregor H, Ellestad G, Cowling R (2002) A continuous fluorimetric assay for tumor necrosis factor-α converting enzyme. Anal Biochem 302:269-275.

Karkkainen I, Rybnikova E, Pelto-Huikko M, Huovila AP (2000) Metalloprotease-disintegrin (ADAM) genes are widely and differentially expressed in the adult CNS. Mol Cell Neurosci 15:547–560.

Kasuga K, Kaneko H, Nishizawa M, Onodera O, Ikeuchi T (2007) Generation of intracellular domain of insulin receptor tyrosine kinase by γ-secretase. Biochem Biophys Res Commun 360:90-96.

Kawachi H, Tamura H, Watakabe I, Shintani T, Maeda N, Noda M (1999) Protein tyrosine phosphatase □/RPTP□ interacts with PSD-95/SAP90 family. Mol Brain Res 72:47-54.

Kawachi H, Fujikawa A, Maeda N, Noda M (2001) Identification of GIT1/Cat-1 as a substrate molecule of protein tyrosine phosphatase ζ/β by the yeast substrate-trapping system. Proc Natl Acad Sci USA 98:6593-6598.

Kim CH, Lisman JE (1999) A role of actin filament in synaptic transmission and long-term potentiation. J Neurosci 19:4314-4324.

Krueger NX, Saito H (1992) A human transmembrane protein-tyrosine-phosphatase,

PTPζ, is expressed in brain and has an N-terminal receptor domain homologous to carbonic anhydrases. Proc Natl Acad Sci USA 89:7417-7421.

Levy JB, Canoll PD, Silvennoinen O, Barnea G, Morse B, Honegger AM, Huang JT, Cannizzaro LA, Park SH, Druck T, Huebner K, Sap J, Ehrlich M, Musacchio JM, Schlessinger J (1993) The cloning of a receptor-type protein tyrosine phosphatase expressed in the central nervous system. J Biol Chem 268:10573-10581.

Li J, Tullai JW, Yu WH, Salton SRJ (1998) Regulated expression during development and following sciatic nerve injury of mRNAs encoding the receptor tyrosine phosphatase HPTPζ/RPTPβ. Mol Brain Res 60:77-88.

Lin Y, Jover-Mengual T,Wong J, Bennett MV, Zukin RS (2006) PSD-95 and PKC converge in regulating NMDA receptor trafficking and gating. Proc Natl Acad Sci U.S.A. 103, 19902–19907.

Ma L, Huang YZ, Pitcher GM, Valtschanoff JG, Ma YH, Feng LY, Lu B, Xiong WC, Salter MW, Weinberg RJ, Mei L (2003) Ligand-dependent recruitment of the ErbB4 signaling complex into neuronal lipid rafts. J Neurosci 23:3164-3175.

Maeda N, Hamanaka H, Shintani T, Nishiwaki T, Noda M (1994) Multiple receptor-like protein tyrosine phosphatases in the form of chondroitin sulfate proteoglycan. FEBS Lett 354:67-70.

Maeda N, Hamanaka H, Oohira A, Noda M (1995) Purification, characterization and developmental expression of a brain-specific chondroitin sulfate proteoglycan, 6B4 proteoglycan/phosphacan. Neuroscience 67:23-35.

Majeti R, Xu Z, Parslow TG, Olson JL, Daikh DI, Killeen N, Weiss A (2000) An inactivating point mutation in the inhibitory wedge of CD45 causes

lymphoproliferation and autoimmunity. Cell 103:1059-1070.

Maurel P, Rauch U, Flad M, Margolis RK, Margolis RU (1994) Phosphacan, a chondroitin sulfate proteoglycan of brain that interacts with neurons and neural cell-adhesion molecules, is an extracellular variant of a receptor-type protein tyrosine phosphatase. Proc Natl Acad Sci USA 91:2512-2516.

Meighan SE, Meighan PC, Choudhury P, Davis CJ, Olson ML, Zornes PA, Wright JW, Harding JW (2006) Effects of extracellular matrixdegrading proteases matrix metalloproteinases 3 and 9 on spatial learning and synaptic plasticity. J Neurochem 96:1227–1241.

Migaud M, Charlesworth P, Dempster M, Webster LC, Watabe AM, Makhinson M, He Y, Ramsay MF, Morris RGM, Morrison JH, O'Dell TJ, Grant SGN (1998) Enhanced long-term potentiation and impaired learning in mice with mutant postsynaptic density-95 protein. Nature 396:433-439.

Milev P, Chiba A, Häing M, Rauvala H, Schachner M, Ranscht B, Margolis RK, Margolis RU (1998) High affinity binding and overlapping localization of neurocan and phosphacan/protein-tyrosine phosphatase-ζ/β with tenascin-R, amphoterin, and the heparin-binding growth-associated molecule. J Biol Chem 273:6998-7005.

Murai KK, Misner D, Ranscht B (2002) Contactin supports synaptic plasticity associated with hippocampal long-term depression but not potentiation. Curr Biol 12:181-190.

Muramatsu H, Zou P, Suzuki H, Oda Y, Chen GY, Sakaguchi N, Sakuma S, Maeda N, Noda M, Takada Y, Muramatsu T (2004) $\alpha_4\beta_1$- and $\alpha_6\beta_1$-integrins are functional receptors for midkine, a heparin-binding growth factor. J Cell Sci

117:5405-5415.

Nagy V, Bozdagi O, Matynia A, Balcerzyk M, Okulski P, Dzwonek J, Costa RM, Silva AJ, Kaczmarek L, Huntley GW (2006) Matrix metalloproteinase-9 is required for hippocampal late-phase long-term potentiation and memory. J Neurosci 26:1923-1934.

Nam HJ, Poy F, Krueger NX, Saito H, Frederick CA(1999) Crystal structure of the tandem phosphatase domains of RPTP LAR. Cell 97:449–457.

Ni CY, Murphy MP, Golde TE, Carpenter G (2001) γ-secretase cleavage and nuclear localization of ErbB-4 receptor tyrosine kinase. Science 294:2179-2181.

Niisato K, Fujikawa A, Komai S, Shintani T, Watanabe E, Sakaguchi G, Katsuura G, Manabe T, Noda M (2005) Age-dependent enhancement of hippocampal long-term potentiation and impairment of spatial learning through the rho-associated kinase pathway in protein tyrosine phosphatase receptor type Z-deficient mice. J Neurosci 25:1081-1088.

Nishiwaki T, Maeda N, Noda M (1998) Characterization and developmental regulation of proteoglycan-type protein tyrosine phosphatase ζ/RPTP β isoforms. J Biochem 123:458-467.

Onyango P, Lubyova B, Gardellin P, Kurzbauer R, Weith A (1998) Molecular cloning and expression analysis of five novel genes in chromosome 1p36. Genomics 50:187-198.

Peiretti F, Deprez-Beauclair P, Bonardo B, Aubert H, Juhan-Vague I, Nalbone G (2003) Identification of SAP97 as an intracellular binding partner of TACE. J Cell Sci 116:1949-1957.

Peles E, Nativ M, Campbell PL, Sakurai T, Martinez R, Lev S, Clary DO, Schilling J,

Barnea G, Plowman GD, Grumet M, Schlessinger J (1995) The carbonic anhydrase domain of receptor tyrosine phosphatase β is a functional ligand for the axonal cell recognition molecule contactin. Cell 82:251-260.

Peles E, Schlessinger J, Grumet M (1998) Multi-ligand interactions with receptor-like protein tyrosine phosphatase β: implications for intercellular signaling. TIBS 23: 121-124.

Postina R, Schroeder A, Dewachter I, Bohl J, Schmitt U, Kojro E, Prinzen C, Endres K, Hiemke C, Blessing M, Flamez P, Dequenne A, Godaux E, van Leuven F, Fahrenholz F (2004) A disintegrinmetalloproteinase prevents amyloid plaque formation and hippocampal defects in an Alzheimer disease mouse model. J Clin Invest 113:1456–1464.

Prybylowski K, Chang K, Sans N, Kan L, Vicini S,Wenthold RJ (2005) The synaptic localization of NR2B-containing NMDA receptors is controlled by interactions with PDZ proteins and AP-2. Neuron 47, 845–857.

Qian Z, Gilbert ME, Colicos MA, Kandel ER, Kuhl D (1993) Tissue-plasminogen activator is induced as an immediate-early gene during seizure, kindling and long-term potentiation. Nature 361:453-457.

Ramos-DeSimone N, Hahn-Dantona E, Sipley J, Nagase H, French DL, Quigley JP (1999) Activation of matrix metalloproteinase-9 (MMP-9) via a converging plasmin/stromelysin-1 cascade enhances tumor cell invasion. J Biol Chem 274:13066-13076.

Reymann KG, Frey JU (2007) The late maintenance of hippocampal LTP: requirements, phases, 'synaptic tagging', 'late-associativity' and implications. Neuropharmacology 52:24-40.

Rio C, Buxbaum JD, Peschon JJ, Corfas G (2000) Tumor necrosis factor-alpha-converting enzyme is required for cleavage of erbB4/HER4. J Biol Chem 275:10379-10387.

Roche KW, Standley S, McCallum J, Dune Ly C, Ehlers MD, Wenthold RJ (2001) Molecular determinants of NMDA receptor internalization. Nat Neurosci 4, 794–802.

Sakurai T, Friedlander DR, Grumet M (1996) Expression of polypeptide variants of receptor-type protein tyrosine phosphatase β: the secreted form, phosphacan, increases dramatically during embryonic development and modulates glial cell behavior in vitro. J Neurosci Res 43:694-706.

Sardi SP, Murtie J, Koirala S, Patten BA, Corfas G (2006) Presenilin-dependent ErbB4 nuclear signaling regulates the timing of astrogenesis in the developing brain. Cell 127:185-197.

Selkoe D, Kopan R (2003) Notch and presenilin: regulated intramembrane proteolysis links development and degeneration. Annu Rev Neurosci 26:565-597.

Shintani T, Watanabe E, Maeda N, Noda M (1998) Neurons as well as astrocytes express proteoglycan-type protein tyrosine phosphatase ζ/RPTP β: analysis of mice in which the *PTPζ/RPTPβ* gene was replaced with the *LacZ* gene. Neurosci Lett 247:135-138.

Skovronsky DM, Fath S, Lee VM, Milla ME (2001) Neuronal localization of the TNFα converting enzyme (TACE) in brain tissue and its correlation to amyloid plaques. J. Neurobiol. 49, 40–46

Streuli M, Krueger NX, Ariniello PD, Tang M, Munro JM, Blattler WA, Adler DA, Disteche CM, Saito H (1992) Expression of the receptor-linked protein tyrosine

phosphatase LAR: proteolytic cleavage and shedding of the CAM-like extracellular region. EMBO J 11:897-907.

Suzuki R, Shintani T, Sakuta H, Kato A, Ohkawara T, Osumi N, Noda M (2000) Identification of RALDH-3, a novel retinaldehyde dehydrogenase, expressed in the ventral region of the retina. Mech Dev 98:37-50.

Tamura H, Fukada M, Fujikawa A, Noda M (2006) Protein tyrosine phosphatase receptor type Z is involved in hippocampus-dependent memory formation through dephosphorylation at Y1105 on p190 RhoGAP. Neurosci Lett 399:33-38.

Turner PR, O'Connor K, Tate WP, Abraham WC (2003) Roles of amyloid precursor protein and its fragments in regulating neural activity, plasticity and memory. Prog Neurobiol 70:1–32.

Tonks NK (2006) Protein tyrosine phosphatases: from genes, to function, to disease. Nat Rev Mol Cell Biol 7:833-846.

Uhm JH, Dooley NP, Oh LY, Yong VW (1998) Oligodendrocytes utilize a matrix metalloproteinase, MMP-9, to extend processes along an astrocyte extracellular matrix. Glia 22:53–63.

Wang J, Tsirka SE (2005) Neuroprotection by inhibition of matrix metalloproteinases in a mouse model of intracerebral haemorrhage. Brain 128:1622-1633.

Wong ST, Winchell LF, McCune BK, Earp HS, Teixidó J, Massagué J, Herman B, Lee DC (1989) The TGF-alpha precursor expressed on the cell surface binds to the EGF receptor on adjacent cells, leading to signal transduction. Cell 56:495-506.

Wu YP, Siao CJ, Lu W, Sung TC, Frohman MA, Milev P, Bugge TH, Degen JL, Levine JM, Margolis RU, Tsirka SE (2000) The tissue plasminogen activator

(tPA)/plasmin extracellular proteolytic system regulates seizure-induced hippocampal mossy fiber outgrowth through a proteoglycan Substrate. J Cell Biol 148:1295-1304.

Yang P, Baker KA, Hagg T (2006) The ADAMs family: coordinators of nervous system development, plasticity and repair. Prog Neurobiol 79:73-94.

Yang H, Jiang D, Li W, Liang J, Gentry LE, Brattain MG (2000) Defective cleavage of membrane bound TGFα leads to enhanced activation of the EGF receptor in malignant cells. Oncogene 19:1901-1914.

Yong VW, Power C, Forsyth P, Edwards DR (2001) Metalloproteinases in biology and pathology of the nervous system. Nat Rev Neurosci 2:502–511.

Yuan W, Matthews RT, Sandy JD, Gottschall PE (2002) Association between protease-specific proteolytic cleavage of brevican and synaptic loss in the dentate gyrus of kainate-treated rats. Neuroscience 114:1091-1101.